NZIC Chemistry IN NEW ZEALAND

ISSN 0110-5566 (Print) ISSN 2624-1161 (Online) Volume 84, No.2, April 2020

Published on behalf of the New Zealand Institute of Chemistry in January, April, July and October.

The New Zealand Institute of Chemistry Incorporated

PO Box 13798
Johnsonville
Wellington 6440

Email: nzic.office@gmail.com

Editor

Dr Catherine Nicholson

C/- BRANZ, Private Bag 50 908
Porirua 5240

Phone: 04 238 1329
Mobile: 027 348 7528

Email: catherine.nicholson@branz.co.nz

Publisher

Rebecca Hurrell

Email: rebeccajhurrell@gmail.com

Advertising Sales

Email: rebeccajhurrell@gmail.com

Printed by Graphic Press

Disclaimer

The views and opinions expressed in Chemistry in New Zealand are those of the individual authors and are not necessarily those of the publisher, the Editorial Board or the New Zealand Institute of Chemistry. Whilst the publisher has taken every precaution to ensure the total accuracy of material contained in Chemistry in New Zealand, no responsibility for errors or omissions will be accepted.

NZIC Chemistry IN NEW ZEALAND

Volume 84, No.2, April 2020

Articles and features

Other columns

Comment from the President

Welcome to the April 2020 issue of *Chemistry in New Zealand*. The NZIC Council had its first meeting of the year in Auckland in February. It was a pleasure to welcome all the new representatives onto Council for 2020 including our Vice-President **Michael Mucalo**. We have already been working productively on a number of issues and I look forward to the rest of the year. It was also a pleasure to welcome **Ian Torrie** to the meeting. Ian is co-chair of the Secondary Chemistry Educators of NZ (SCENZ) group, and has been very active recently responding to the proposed changes to NCEA. This is an ongoing process. The rest of the Council meetings will take place using digital technology to ensure we keep costs down. The meetings will also be shorter and more focussed to enable action items to be achieved.

I attended the 18th Asian Chemical Congress (ACC) in Taiwan in December and also represented the NZIC at the **20th General Assembly of the Federation of Asian Chemical Societies (FACS)**. It was a privilege to be present to see **David Warren** be awarded his **education medal**. The general assembly was productive and I will be working with representatives from Australia to streamline the application process for the FACS awards, empowering more NZ researchers to apply for these prestigious awards by making the application process (hopefully) a lot clearer.

A new initiative is the inaugural Commonwealth Chemistry Congress which should have taken place in Trinidad and Tobago in May. Unfortunately, due to COVID-19, the executive board has taken the tough but correct decision to postpone the congress until the start of 2021. Regardless, we are delighted to have three representatives from New Zealand represent NZIC at this congress: **Anna Garden** (Otago), **Catherine Whitby** (Manawatu) and **Sangata Kaufononga** (Waikato). I will also be attending, having been elected to the executive board of Commonwealth Chemistry, the Federation of Commonwealth Chemical Sciences Societies. This is a great privilege and I am looking forward to working with the other executive board members and leading initiatives in this space.

As I write, the **Pacifichem** congress is still scheduled to go ahead as planned. Abstracts are coming in fast and hopefully we will have a strong representation from New Zealand.

Domestically I am in conversation with the branch secretaries to travel to the branch centres to give the president's talk. I am really looking forward to connecting with you all again after meeting so many of you at the NZIC conference last year.

A reminder that applications for the NZIC prizes will close on 30 June. In 2020 we have the following prizes available: the **Maurice Wilkins Centre Prize for Chemical Science**, the **Shimadzu Prize for Industrial and Applied Chemistry**, the **Denis Hogan Chemical Education Award sponsored by sciPad**, and the new **Brian Halton Award**

for the best paper in the field of chemistry published by a New Zealand university student. For more information and how to apply please go to the media hub section of the NZIC website.

Finally, this will be the last edition of *Chemistry in New Zealand* that is produced by **Rebecca Hurrell**. Becs is stepping down from the role after 15 years. On behalf of the NZIC and all who are involved in bringing *Chemistry in New Zealand* together, a huge THANK YOU Becs for your hard work, initiative and cheerful communication over the years. We wish you well with your future endeavours.

Sarah Masters

NZIC President

From the Editor

After 15 years in the role, Rebecca Hurrell has decided to step down as publisher for *Chemistry in New Zealand*. On behalf of NZIC, I'd like to thank Becs for all the work she has done in putting each issue of the journal together. On a personal note, I have always appreciated the enthusiasm she has brought to the job, not only in terms of the publishing process but also in answering queries of all kinds related to both the journal specifically and NZIC matters more generally. We wish Becs all the very best.

We are now on the lookout for someone to take up this vacant role. If you are interested, please get in touch for more information.

Catherine Nicholson

Editor

New Zealand Institute of Chemistry

supporting chemical sciences

April News

AUCKLAND

The University of Auckland

Events

The IUPAC Global Women`s Breakfast was held on 12 February at the University. Auckland kick-started the event which took place in 200 locations around the globe.

School of Chemical Sciences seminars

The School of Chemical Sciences has hosted several seminars already this year:

Dr Frank Petersen (Novatis, Switzerland): *Natural product sciences in modern drug discovery and paths to the future*

Professor Rhett Kempe (University of Bayreuth, Germany): *Green chemical science by catalysis*

Dr *Davide* ***Mercadante***: *Structures through the computational microscope: achievements and challenges in understanding macromolecular dynamics in the era of digitalization.*

Valedictory Lecture

Professor *Ralph* ***Cooney***: *A long research journey into the era of climate change*. His talk covered his five decades in research and academic leadership roles around the world.

NZIC Auckland Branch Seminars

The University of Auckland hosted the following Branch Seminars in January and February 2020:

Professor David Kingston (Virginia Tech): *The history, chemistry, and biology of paclitaxel, an anticancer gift from Nature*

IUPAC Global Women's Breakfast 2020

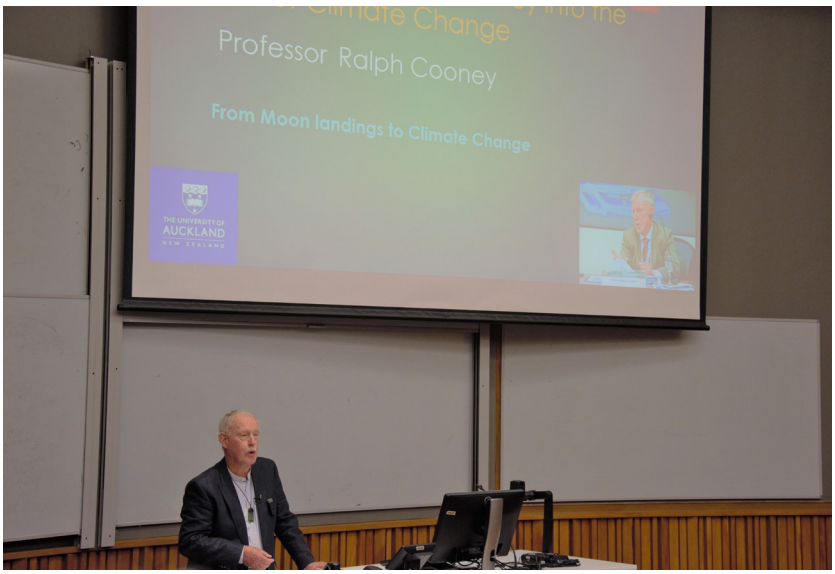

Ralph Cooney's valedictory seminar at The University of Auckland

Dr Love-Ese Chile (Grey to Green Sustainable Solutions, Vancouver, Canada): *Advocacy, education and research to build a circular bioeconomy for plastics*

Staff Successes

Rebecca ***Deed***, Lecturer in Wine Science, was selected to be a Panel Leader to run a team of wine judges at the Royal Easter Show Wine Awards 2020.

Jianyong ***Jin*** and his polymers group were featured in *Uni News* with an item discussing their recent research on visible light-based 3D printing of living polymers, enabled by incorporation of photo-RAFT agents. For more information see: *www.auckland.ac.nz/en/news/2020/01/16/Researchersprintlivingself-repairing-plastics.html*

Congratulations to Dr *Davide* ***Mercadante*** for becoming a topic editor for the journal *Frontiers in Molecular Biosciences*. Together with a team of editors including researchers from Novozymes and The University of Copenhagen in Denmark, Stony Brooks University in New York and Nainjin University in China, Dr ***Mercadante*** will lead the publication of a topic issue treating the subject of *advanced sampling and modeling in molecular simulations for slow and large-scale molecular dynamics*.

Publications

Matthew P. Sullivan, Michael Groessl, Samuel M. Meier, Richard L. Kingston, David C. Goldstone, Christian G. Hartinger*, *The metalation of hen egg white lysozyme impacts protein stability as shown by ion mobility mass spectrometry, differential scanning calorimetry, and X-ray crystallography,* Chemical Communications, 2017, 53(30), 4246-4249.

Matthew P. Sullivan, Michél K. Nieuwoudt, Nelson Y. S. Lam, Dianna Truong, David C. Goldstone, Christian G. Hartinger*, *Unexpected arene ligand exchange results in the oxidation of an organoruthenium anticancer agent: the first X-ray structure of a protein–Ru(carbene) adduct* Chemical Communications, 2018, 54(48), 6120–6123.

Student Successes

PhD Completions

Congratulations to Matthew Sullivan for successfully defending his PhD entitled, *Metallodrugs and proteins: expanding the bioanalytical toolkit to investigate the metallation of biomolecules*. Matthew was supervised by *Christian* ***Hartinger*** and *David* ***Goldstone***.

Congratulations to Buzhe Xu for successfully defending his PhD thesis entitled, *Total synthesis of naturally occurring antimicrobial peptides*. Buzhe was supervised by Distinguished Professor Dame *Margaret* ***Brimble*** and Associate Professor *Paul* ***Harris***.

PhD Student Prizes

Congratulations to PhD student Andrew Chan (working with *Ben* ***Mallet***, *Cather* ***Simpson*** and *Tilo* ***Söhnel***) who won best student talk at the 44th Condensed Matter and Materials

Meeting that was held 4-7 February in Rotorua.

Congratulations to PhD student Sneh Patel (working with *Tilo* ***Söhnel***) who won best student poster at the 44th Condensed Matter and Materials Meeting and also won the first-ever meme competition and became the meme master of the conference.

Congratulations to Danny McDougall who won second prize at the NZ Trace Elements Group conference in Cambridge for his talk entitled, *Trace metals in New Zealand green-lipped mussels and the effect of water treatment on trace metal bioavailability and mussel survival*.

Polymers group 2020

Massey University

Events

Associate Professor *John* ***Harrison*** and Dr *Marie-Anne* ***Thelen*** welcome Kai Dollevoert from the University of Amsterdam for a six months internship where he will be developing analytical methods for heavy metal analysis.

Dr *Debbie* ***Jordan***, *Erin* ***Moffet*** and *Jade* ***Pope*** hosted 180 Year 13 students from all around New Zealand at the annual Rotary Science Forum held in Auckland over two weeks in January. The students mastered the art of separation using recrystallisation of a natural product and the distillation of alcohol from wine. Then they applied high school knowledge to explosive reactions!

Dr *Jon* ***Kitchen*** hosted Professor Annie Powell and PhD student Anthony Carter from Karlsruhe Institute of Technology as part of a Strategic Research Excellence Fund collaborative project looking at surface immobilised molecular magnets. Otago PhD student Sriram Sundaresan also visited Massey to carry out Langmuir-Blodgett deposition of his multifunctional, switchable materials.

Chemistry won the pavlova making competition at the School of Natural and Computational Sciences Christmas Party in December with our periodic table themed entry (technically not a pavlova, but it was pretty cool!)

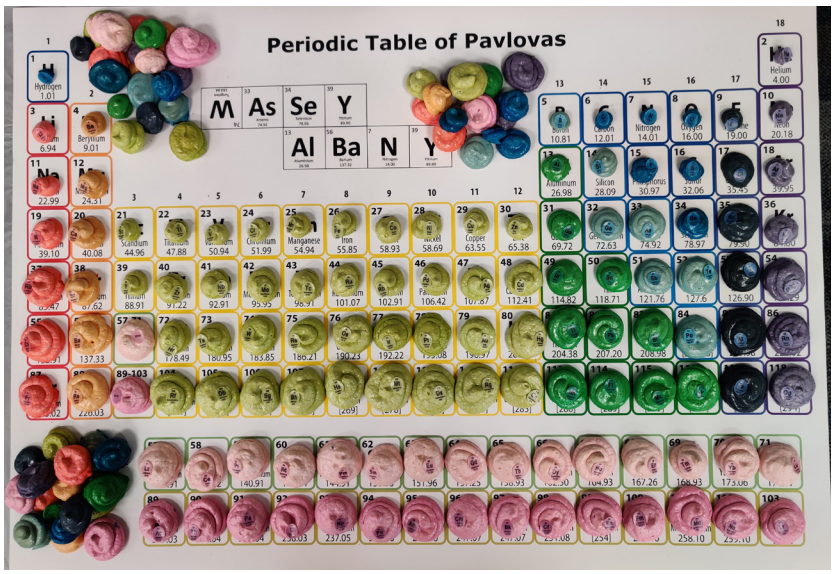

Periodic table themed “pavlova”

Seminars

In December Distinguished Professor *Peter* ***Schwerdtfeger*** gave a public lecture on the periodic table entitled, *The periodic table From a quantum perspective* as part of the Massey Fascination Science lecture series.

Student successes

Congratulations to Jade Pope (PhD with *John* ***Harrison***) who is the recipient of a Vice Chancellor’s Doctoral Scholarship.

AUT

New Faces

We welcome Dr *Cassandra* ***Fleming***, our new lecturer in chemistry who joined us in January. Cassandra competed her PhD at Deakin University (Australia), after which she moved to Sweden for postdoctoral work with Professor Joakim Andréasson (Chalmers University of Technology) and Professor Morten Grøtli (University of Gothenburg). Cassandra’s research interests include light-controlled enzyme inhibition, the development of light-responsive drug delivery systems and fluorescent bioactives to probe dynamic biological functions.

Andres Tiban Anrango joins us for a PhD under the supervision of Dr *Jack*

Chen. Andres is working on the development of cellulose particles for surfactant applications and is funded by a SfTI Seed Project.

We welcome back Jess Frederickson who will be starting an Honours project with Professor *Nicola* ***Brasch***.

Events and Invited Talks

To celebrate the 150th birthday of the periodic table, the NZIC Auckland Branch hosted Dr Eric Scerri (UCLA), a world authority on the history and philosophy of the periodic table. His lecture entitled, *The periodic table, its story & its significance* gave a historical tour of important steps in the evolution of the periodic table and suggested moving to an 18 column periodic table!

Dr Jack *Chen* and his PhD students Pablo Solís Muñana and Chloe Zhijun Ren each gave talks at the NZIC conference in Christchurch. Pablo and Chloe's travel were supported by travel grants from the NZIC.

Jack Chen with PhD students Pablo Solís Muñana and Chloe Zhijun Ren

CANTERBURY

The annual BBQ was held on 26 February at the University of Canterbury Club, Ilam Homestead.

The great migration is (almost) complete

Most of the School of Physical and Chemical Sciences staff at UC migrated out of the West (old Rutherford) building at the end of 2019. Chemistry staff offices are now to be found in the Beatrice Tinsley building which was opened by Hon Dr Megan Woods, Minister of Research, Science and Innovation, Vice-Chancellor Cheryl de la Rey and Pro-Vice Chancellor Science Professor Wendy Lawson, in front of 130 guests including members of Beatrice Tinsley's family, some of whom travelled from the United States to be there. UC alumna Beatrice Tinsley (1941 – 1981) is known as one of the most creative and significant theoreticians in modern astronomy. She graduated from UC with a Bachelor of Science degree (1961) and Master of Science in physics with First Class Honours (1963) before going on to complete a doctorate at the University of Texas and take up a Professorial role at Yale University, becoming the university's first female Professor of Astronomy. Beatrice Tinsley was a role model and mentor to many New Zealand and American women during her academic career. The opening of the building completed the Regional Science and Innovation Centre at UC with the building being connected to both the Ernest Rutherford building (which houses undergraduate labs and postgraduate spaces) and the Julius von Haast building.

Winners at UC 2019

The superb talents of many students of chemistry at the University of Canterbury were acknowledged with the award of annual prizes for excellence in Chemistry. The 2019 winners were:

The New Zealand Institute of Chemistry Prize: *Toby* ***McDonald*** and *Jude* ***Kalan***

Haydon Prize for Chemistry: *Rachael* ***Cleave*** and *Keat* ***Beamsley***

Ralph H Earle Jnr Seminar Prize: *Ben* ***Howard***

C.E. Fenwick Prizes in Chemistry: *James* ***Kolien***

C.E. Fenwick Prizes in Chemistry: *Jordan* ***McIvor***

Jack Fergusson Prize: *Ezra* ***Prattley***

The IUPAC Global Women's Breakfast

The Canterbury branch of NZIC hosted the IUPAC Global Women's Breakfast event at UC on the morning of 12 February, following on from the International Day of Women and Girls in Science day. The event was well attended. It was wonderful to see a broad range of employment, culture, gender and backgrounds represented at the breakfast. We were grateful to have our guest speaker, Associate Professor Catherine Bishop (UC Mechanical Engineering) give her insight into studying and working in different places and cultures and also to Gail Route (Te Kura School) for her appropriate karakia for the meeting. We had a great discussion and were very fortunate to have an online chat with Professor Mary Garson AM who led the planning and coordination of global activities for the celebration

The opening of the Beatrice Tinsley Building

Participants in the Global Women's Breakfast

of IUPAC100 in 2019 and instigated the Global Women's Breakfast movement. Our only disappointment is that, in having our event so early and being the first place in the world, we do not get to "touch hands" with many other groups around the rest of the world. We are cheekily suggesting that we'll see if we can do a Global Women's cocktail hour next year and the idea has already been floated to Mary and her co-organiser Laura! *Sarah* ***Masters*** was, however, able to connect with the final breakfast in Hawaii, closing the loop for 2020 of breakfasts around the world. We were not able to get a photograph on the day but later rustled up as many attendees as we could later in the week!!

Erskine visitors to UC

The University of Canterbury welcomes Erskine/Oxford/Cambridge visitors each year and this year we have Professor Ed Constable (Basel, Switzerland), Professor Martin Castell (Oxford, UK) and Professor Torsten Berger (Vienna, Austria) visiting us. The bequest by John Angus Erskine enables up to 70 visiting international senior academics to lecture at UC each year to undergraduates and postgraduate students. The visitors are getting stuck into their teaching and will be doing some lectures for NZIC during their visit here.

MANAWATU

We would like to welcome *Lauren* ***Macreadie***, the new chemistry lecturer at Massey University in Palmerston North. Lauren completed a double degree in biomedical science/science at Monash University in Melbourne, Australia. She then went on to complete her PhD at CSIRO and Monash University. Lauren moved to Trinity College Dublin as a joint postdoctoral/teaching fellow for a year before moving back to CSIRO in Melbourne to work on commercial MOF projects. Following this role, Lauren arrived at Massey University as a postdoctoral fellow and was then appointed as a chemistry lecturer.

We also welcome *Ayiya* ***Bikimi***, the new chemistry lecturer at UCOL. Ayiya is originally from Nigeria and immigrated to New Zealand in 2015 to pursue a doctorate degree at the University of Auckland under the supervision of Prof. *L. James* ***Wright***. Ayiya holds a Bachelor of Technology (Hons) in industrial chemistry from Abubakar Tafawa Balewa University, Bauchi-Nigeria. He then went on to completed a Master of Science in petroleum technology from the University of Teesside, Middlesbrough, England. Over the years, his research has been strongly focused on the synthesis and design of the newly developed pyridylidene amides with amidate and remote or mesoionic N-heterocyclic carbene donor function alongside their applications as metal supports for catalysis. In July 2019, he was appointed as a lecturer in the Applied Science team at UCOL teaching chemistry.

Victoria-Jayne Reid joined the ***Telfer*** group as part of a summer internship.

Omid ***Taheri*** graduated with his PhD on gas separations by MOFs and was placed on the Dean's List of exceptional theses. He has since headed off to a postdoctoral position at the University of Manchester, UK.

The NZIC Manawatu Branch organised a breakfast to celebrate Women in Chemistry on 12 February. Over 25 people attended the breakfast held at Moxxies, Palmerston North. Esther Hutchinson from Synlait spoke about

her extended experience working in the chemistry industry.

MOF aficionados from around NZ descended in Queenstown on 10-11 February for a mini conference with international colleagues.

Distinguished McKnight University Professor Natalia Tretyakova from the University of Minnesota gave a lecture titled, *DNA-protein cross linking at epigenetic marks of DNA* on 31 Jan.

Dr *David* ***McMorran*** from the University of Otago gave a lecture entitled, *Two stories in metallosupramolecular chemistry* on 4 December.

Paul ***Plieger*** attended ACC18 (Asian Chemical Congress) in Taipei, Taiwan in mid-December. This larger conference (over 2000 delegates) is a biennial event organised by members of the Federation of Asian Chemical Societies (FACS). Paul presented his group's recent results on second-sphere stabilisation of beryllium coordination compounds. While there, he also represented the NZIC on the Asian Chemical Editorial societies (ACES) board and co-chaired the ACES-GDCh symposium. Also in early January, the ***Plieger*** group celebrated first published papers for *Tyson* ***Dais***, *David* ***Nixon***, *Becky* ***Severinsen*** and *Sidney* ***Woodhouse*** and the recent promotion of Paul to Professor.

A large contingent of Manawatu Branch members from Massey University attended the NZIC 2019 conference in November.

Manawatu Branch members at the NZIC Conference dinner. Front row, left to right: Sidney Woodhouse, Mark Waterland, Vyacheslav Filichev, Yongdong Su, Harikrishnan Mohana Kurup, Marryllyn Emma Donaldson, Rebecca Severinsen.

Back row, left to right: Bruce Chilton, Adil Alkas, Suraj Patel, Tyson Dais, Leonie Etheridge, Geoff Jameson, Arka Gupta, David Harding.

2020 Hands On at Otago Natural Products Chemistry project participants

OTAGO

University of Otago, Department of Chemistry

Each year, Otago University welcomes over 400 high school students from around the country for a week-long chance to experience university-level research and teaching through Hands On at Otago. Sixteen of these students chose to spend each morning taking part in a Natural Products Chemistry project, where they used caffeine as a case study to explore methods of isolation, characterisation and synthesis in organic chemistry. A large number of other students spent an afternoon carrying out a smaller chemistry 'snack', which involved either preparing and studying nanoparticles or carrying out a synthesis of a coordination complex. These projects were led by *Dave* ***McMorran***, *Dave* ***Warren*** and a number of chemistry department graduate students.

Alistair ***Richardson*** successfully defended his PhD thesis entitled, *Chemistry of a stable vitamin C glycoside in apples (Malus spp.) and other fruit crops* supervised by *Nigel* ***Perry*** and *Dave* ***Larsen***, with assistance from Plant & Food Research staff at Hawkes Bay, Palmerston North and Clyde. Alistair is now working in *Emily* ***Parker***'s group at Victoria University Wellington.

In February, Professor David Kingston of Virginia Tech visited the Department and delivered a fascinating talk about the history of paclitaxel (Taxol) for cancer treatment. Also visiting were Dr Sharali Malik and Professor Annie Powell of Karlsruhe Institute of Technology, speaking about carbon nanotubes and iron chemistry, respectively.

Jaydee ***Cabral*** presented at the Tissue Engineering & Regenerative Medicine Conference in Orlando, Florida, USA, Dec 2-5, 2019.

The group of *Anna* ***Garden*** welcomed three new students; *Frank* ***MacKenzie*** (working towards a BSc(Hons) and *Sam* ***McIntyre*** and *Ciaran* ***Ward***, both MSc students. All the best with your new projects, everyone!

Sara ***Miller*** has started exploring the use of spectroscopic techniques to diagnose gastrointestinal diseases *in vivo*, via endoscopy, to minimise the need for biopsy collection. This research is being supported by the complementary MBIE Smart Ideas and Marsden Fast-Start grants. These studies are being carried out in collaboration with colleagues in the Dunedin School of Medicine, University of Auckland and University of Exeter.

Keith ***Gordon*** has recently completed the second part of his Royal Society of Chemistry Australasian tour where he spoke at the University of Adelaide, Monash and University of Melbourne.

Alongside these achievements, members of the ***Gordon*** group have been, or will be, busy attending a range of conferences. *Samanali Garagoda* ***Arachchige*** gave a talk at the Asia-Pacific Optical Sensors Conference in Auckland on her work into identifying graphene treated textiles using Raman spectroscopy combined with chemomerics, while *Joseph* ***Mapley*** spoke at the Australasian Community for Advanced Organic Semiconductors in Katoomba about his study into the electronics of porhyrin ferrocenes tuned with electron withdrawing groups. *Fatema* ***Ahmmed*** recently gave a talk at World Congress on Oils and Fats 2020 in Sydney on her work examining krill oils using Raman and IR spectroscopy.

A number of papers have recently been produced by the group. *Chima* ***Robert****'s* paper on *Rapid discrimination of red meat types using Raman spectroscopy* has been submitted to *Journal of Food Chemistry*. *Samanali Garagoda* ***Arachchige***'s paper, *Understanding consolidants on Harakeke fibres using Raman microscopy; implications for conservation*, has been accepted by *Journal of Cultural Heritage*. *Fatema* ***Ahmmed***'s paper, *Marine omega-3 phospholipid. A comprehensive review of their properties, sources, bioavailability and relation to brain health* was published in *Comprehensive Reviews in Food Science and Food Safety*. *Joe* ***Mapley*** has recently submitted the paper, *Investigation of ferrocenelLinkers in β-substituted porphyrins* to *Journal of Physical Chemistry A*. *Kārlis* ***Bērziņš*** published a paper titled, *Low-wavenumber Raman spectral database of pharmaceutical excipients* in *Vibrational Spectroscopy*.

Sung Jun ***Lim*** is a visiting student from UNIST (Ulsan National Institute of Science and Technology), Ulsan, South Korea. He is visiting to make some resonance Raman spectroscopy measurements of photosensitive dyes for dye-sensitised solar cells with his supervisor, Professor Tae-Hyuk Kwon.

The ***Gordon*** group welcomes back *Jacob* ***Harrison*** for a one year Masters looking at a range of donor-acceptor dyes.

WAIKATO

The new Waikato branch committee for 2020 is as follows:

Chairperson: *Bill* ***Henderson***

Secretary: *Lewis* ***Dean***

Treasurer: *Jo* ***Lane***

Council Delegate/ Branch editor: *Michèle* ***Prinsep***

Student representative: *Nyssa* ***Hewitt***

Ordinary members: *Michael* ***Mucalo***, *Megan* ***Grainger***, *Ingrid* ***Lindeman***, *Jacob* ***Shrubsall***

The winners of the undergraduate chemistry prizes for 2019 were as follows:

J.E. Allan Memorial prize (for best overall student at second year): *Siyuan* ***Li***

Prize for best overall student at third year: *Edie* ***Thomas***

Winners of the chemistry writing competition sponsored by the branch were:

1st prize: *Claire* ***Voogt***

Second equal: *Lewis* ***Dean*** and *Zahida* ***Zia***

Around fifteen people attended a very enjoyable breakfast that was held at Jack's Coffee Lounge, Hamilton in February as part of the Global Women's Breakfast event for female chemists. After the great success of the IUPAC inaugural event in 2019, it was decided to run the event again in 2020.

University of Waikato

Two of our doctoral students, Haiming Tang and Sangata Kaufononga, had their degrees conferred at a recent ceremony. Haiming's thesis (*The coordination chemistry of S/N-donor ligands towards platinum group metals and gold)* was supervised by *Bill* ***Henderson*** and Sangata's thesis (*Indole diterpenoid secondary metabolites produced by the*

Epichloë festucae var. lolii – Lolium perenne symbiosis) was supervised by *Michèle* ***Prinsep*** (with colleagues at AgResearch).

Megan ***Grainger*** had three students working with her over the summer. Hannah Klaus and Edie Thomas were on summer research scholarships working on the elemental profile of honeybees and pesticide analysis in New Zealand and overseas honeys

Hamilton Global Women's breakfast participants

Sangata Kaufononga at graduation with her father (who travelled from Tonga for the ceremony) and her supervisor, Michèle Prinsep

respectively. Shaun McNeil carried out contract research for Contact Energy on mercury in eels from the Waikato River. Hannah spoke at the summer research function about her project and what the opportunity meant for her, whilst Edie's poster was ranked in the top three science research posters.

The University of Waikato hosted the New Zealand Trace Elements Group Conference in February. Three Waikato staff were on the organising committee: *Amanda* ***French*** (Convenor), *Megan* ***Grainger*** and *Adam* ***Hartland***. Keynote speakers were William Maher from the University of Canberra (*Advances in speciation analysis of metalloids by HPLC-ICPMS*), Fui Yuen (Steven) Pang from Agilent Technologies, Singapore (*Reclaim your wasted remeasurement time with a next generation AI-powered ICP-OES*) and Gavin Robinson from PerkinElmer (*Advances and applications of nanoparticle analysis by ICP-MS*). There were a number of other speakers from the Waikato region including students Sebastian Höpker (*Towards quantifying palaeoclimatic cave drip rates from trace metals in stalagmites*), Brittany Ward (*Assessing deglacial Southern Hemisphere Westley Wind behaviour using speleothem trace element measurements*), Sukhjeet Singh (*Novel gas use for spectral interference reduction of sulfur in Inductively Coupled Plasma Mass Spectrometry (ICP-MS)*) and Mahdiyeh Salmanzadeh (*Isotopic differences in cadmium between soil types and land uses*). The prize for the best student presentation was won by Brittany Ward.

Scion

Laura ***Raymond***, *Meeta* ***Patel***, and *Stefan* ***Hill*** have begun a project for the rapid screening of cannabis leaves and buds for cannabinoids currently be utilised in medical and nutraceutical applications and also for those with no current identified use. A combination of targeted and untargeted metabolomics utilising NMR spectroscopy and mass spectrometry is being employed. This study is a joint project between Scion, Rua Bioscience (Manu Caddie), and Auckland Unitec (Gregor Steinhorn and Wayne Holmes). Results from the study will be combined with hyperspectral analysis of cannabis carried out by Auckland Unitec and the University of Waikato (Dr Melanie Ooi).

Eva ***Gaugler*** is working with a Massey University student investigating the migration of non-intentional chemicals from plastics that are to be used in contact with food. To complement this work, Eva has been working with the Australian Government National Measurement Institute developing new methods for the measurement of organic nanoparticles in the biosphere.

Kate ***Parker***, *Meeta* ***Patel***, and *Jamie* ***Bridson*** were involved in a collaborative study with the University of Canterbury, Watercare, and the Auckland Council, which has published findings of a survey of the state of microplastics on beaches in the Auckland region. The results echoed a similar study carried out in Christchurch and highlighted the insidious nature of plastics when they are not appropriately disposed of.

Kendra ***Newick*** visited Professor Neil Ward at the University of Surrey for advanced training on ICP-MS techniques and to finish work started as part of an MBIE Smart Ideas project using 3D printed molecularly imprinted polymers for enhanced toxic trace metals removal from water.

Laura ***Raymond*** recently published a paper outlining the secondary metabolites extracted with supercritical carbon dioxide ($scCO_2$) from hardwood and softwood trees. Understanding the nature of the extracts builds on work where $scCO_2$ has been used to remove water from wood to increase value. This work has shown that there is also value in the removed water 'waste' stream.

Essential B-N interactions in linear and cyclic donor-acceptor complexes: a review

Aliyu M. Ja'o and Sarah L. Masters*

School of Physical and Chemical Sciences, University of Canterbury, Private Bag 4100, Christchurch 8140 (email: *sarah.masters@canterbury.ac.nz*)

Keywords: *B-N interaction, donor-acceptor complex, amine borane, ammonia borane*

Introduction

Donor-acceptor (D–A) complexes, otherwise referred to as Lewis acid-base adducts, are based on the theory of acids and bases developed in 1938 by Gilbert N. Lewis.[1] These complexes have found application as potential hydrogen storage materials,[2-4] advanced materials coatings[5-7] and as precursors in synthetic chemistry.[8-12] Donation and acceptance of electron pairs are the central point of this theory, with the electron-rich base having an electron pair to donate while the electron-deficient acid with an open site in its coordination sphere accepts the electron pair resulting in the formation of a stable complex. This stable complex is called a donor-acceptor complex with the interaction influenced by strong induction and electrostatic forces between the acids and the bases. The stability of these complexes has been shown to rely upon the basicity of the donors (bases).[13] Substitution effects on the individual donor and acceptor compounds also determine the stability of the adduct.[14] For instance, in a theoretical study, it was found that successive methyl substitution on the nitrogen in the donor compound favoured the formation of the complex. However the reverse is the case for the substitution on the boron in the acceptor compound. Complexation results in geometrical variations of the individual monomers. The variations can be linked to the stability and bonding properties of the complexes.[15] These changes can also be justified by means of valence shell electron pair repulsion theory (VSEPR)[16] taking into account that complex formation is driven by transfer of electrons away from the donor.

The donor-acceptor bond (also known as a dative bond) in these systems generally differs from ordinary covalent bonds in that they have lower dissociation energies, a longer bond length and are sensitive to inductive effects. Another distinction between a donor-acceptor bond and a covalent bond is the way the rupture of the bond takes place. An example can be seen in two compounds which are isoelectronically similar: ammonia borane (H_3NBH_3) and ethane (H_3CCH_3). While rupture of the C–C bond in the latter takes place heterolytically, it proceeds homolytically in the former to break the B–N bond.[17] *Ab initio* calculations suggested the dative B–N bond vibration possesses strong anharmonic character indicating the bond is similar to strong van der Waals bonds.[18]

With advanced and sophisticated computing power and improvements to computational methods it is now possible to obtain far more accurate theoretical molecular structures of simple molecules. As a result, gas-phase experimental structure determination can now be undertaken with many assumptions such as symmetry and application of constraints in the structural analysis reduced or eliminated through the use of combined methods such as Molecular Orbital Constrained Electron Diffraction (MOCED)[19] and Structure Analysis Restrained by *Ab initio* Calculations for Electron diffractioN (SARACEN).[20-22] Correlating the chemical properties such as stability and the strength of acid/base with the experimental structural parameters such as the dative bond distance in D–A complexes is essential in understanding the behaviour of D–A complexes.

Amine-borane adducts are a class of Lewis acid-base adducts formed via the formation of a dative bond between an amine and a borane group (see, for example, Eq. 1). The most common example is ammonia borane which had come under extensive investigation due to its potential application as a hydrogen storage material.[23]

$$CH_3NH_2 + \frac{1}{2}B_2H_6 \rightarrow CH_3NH_2\text{–}BH_3 \qquad \text{(Eq. 1.)}$$

Owing to the electron deficiency of borane (BH_3), it becomes stabilised by accepting electrons from the nitrogen atom on amines thereby forming amine-boranes which are relatively stable in the solid phase. This interaction makes amine-boranes more stable with higher melting points than their organic analogues. For instance, ammonia borane NH_3BH_3 is more stable with a higher melting point than ethane.[24] This is also due to the presence of unconventional intramolecular interactions in the former that are absent in the latter. Amine-boranes have been characterised extensively using single-crystal X–ray diffraction (XRD), microwave spectroscopy (MWS), gas-phase electron diffraction (GED) and quantum chemical calculations (QC). However, some amine boranes like ammonia borane are also characterised by low vapour pressure,[2] meaning that elevated temperatures are required to study them in the gas phase. As they have a tendency to dissociate at elevated temperatures,[25] studying them using GED can become very challenging. The dative B–N distance, in particular, has always been of interest since it was observed that dehydrogenation is favoured across this interaction[26] and that methyl-substitution at N enhances the stability of the dative bond by lowering the reaction enthalpy of the dehydrogenation process.[27]

While several forms of Group 13/15 donor-acceptor complexes abound, in this review the focus will be limited to the linear and N–H–containing heterocyclic donor-acceptor complexes formed between nitrogen and boron

atoms. In this review, various different internuclear distance parameters are quoted depending on the structural method used to obtain it, for example, r_g, r_s, r_o etc.[28–31]

Ammonia borane

Amine-based compounds are usually common in the formation of donor-acceptor complexes. Amine-boranes for instance are the most common complexes that have been well studied. This is owing to their applications in various areas of human endeavour, for example as alternative energy[23, 32, 33] and as valuable precursors in synthetic chemistry.[33, 34] Ammonia borane (AB)[35-37] is the most widely known complex in this category, being the simplest amine-borane donor-acceptor complex. It has been well characterised by different techniques. As far back as 1955, Shore and Parry[38] synthesised AB with the molecular weight measurements and crystal structure determined from its X–ray diffraction powder pattern indicating its occurrence as a monomer. The structure of AB with a tetragonal symmetry was, however, incomplete due to the trial and error approach adopted in deriving the indices. Another issue was the presence of two molecules per unit cell with each molecule lying on a four-fold axis in an asymmetric arrangement. AB has a substantial dipole moment and is expected to be polar.[39, 40] Reanalysing the data by employing several factors and considering the fact that calculated intensities points to the polar form, a complete structure based on a body-centred structure with a B–N distance of 156.0 ± 0.05 pm was obtained.[41] Lippert and Lipscomb[42] reported a similar structure but with a B–N distance (*r*B–N = 160.0 ± 0.2 pm) having a larger uncertainty caused by an interaction between scale and temperature factors. Another structure with a face-centred orthorhombic unit cell was later reported.[43] Using powder XRD data, Hoon and Reynhardt[44] found that although AB has a body-centred tetragonal structure at room temperature, at a lower temperature of about 220 K the face-centred orthorhombic form actually exists. A higher temperature *ab initio* molecular dynamics study[45] at 423 K suggested a proton ordered orthorhombic *Pnma* structure as the most stable. However, there were concerns that AB having a flat potential energy surface might make even accurate XRD structures misleading. Bearing this in mind, the XRD structure was re-determined at 200 K which also yielded the orthorhombic form with a B–N separation of 156.4 pm (no uncertainty given).[46] This structure appears to be accurate. For instance, in order to evaluate the reliability, its geometry was fully optimised at MP2(Full)/6-31G* level with the above *r*B–N value frozen resulting in a structure only 6 kJ/mol higher in energy. This difference in energy is within reasonable chemical accuracy (4–8 kJ/mol).[47] As reliable as this structure seems to be, it was observed that the B and N atoms in the previous XRD studies were not assigned appropriately. Therefore, B and N were reassigned in a new neutron crystal study[48] at 200 K thereby obtaining an orthorhombic structure (*Pnma* space group) with a bent B–H…H angle (θ) and linear N–H…H angle (ψ) in the dihydrogen interaction (Fig. 1). The interaction featured a bond length of ~202 pm and a B–N separation of 158.0(2) pm. The reverse was observed in the previous XRD studies.

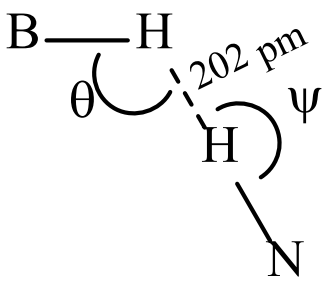

Fig. 1. A schematic diagram showing the B-H…H-N interaction between molecules of ammonia borane

Another XRD study[49] at 90 K which accurately determined the localised hydrogen positions revealed a similar orthorhombic structure as in the neutron crystal study above but with a slightly longer B–N bond [*r*B–N = 159.9(8) pm]. The study found the dihydrogen bond distance to be 191.0 pm which is appreciably lower than the sum of the van der Waals radii of B and N atoms. The same authors observed a tetragonal structure accounting for the degree of disorder of the hydrogens in the molecule with almost similar B–N separation [*r*B–N = 159.7(3) pm] at 298 K.

In the gas phase, AB is characterised by a longer B–N bond as evident in a MWS study[50] which yielded a B–N distance of r_o = 167.2(5) pm and a dipole moment of 5.216(17) D. This is not surprising because, in solids, dipole moment and packing effects have in many cases been responsible for bond shortening.[51] The MWS B–N distance was reproduced accurately by *ab initio* calculation at the MP2(Full)/6-31G level.[46] Corrections based on calculated vibration-rotation constants have been applied to the experimental rotational constants obtained in the above MWS study to derive a semi-experimental structure[52] which was found to be in excellent agreement with the one calculated at CCSD(T) level and basis set extrapolated to the complete basis set limit up to quintuple-ζ quality. These yielded a B–N distance of 164.5(1) pm and 164.5 pm for the former and the latter respectively.

Alkyl-substituted amine-boranes

Structures of methyl-substituted derivatives have been reported with marked structural differences influenced by the phase of the complexes. A comparative structural study in the gas and solid phase of mono-, di- and trimethyl amine boranes [$Me_nH_{3-n}N{\cdot}BH_3$ (n=1–3)][53] indicate longer dative bonds in the gas phase than in solids as shown in Table 1 with the dative bonds associated with large anharmonic vibrations. Thus, vibrational corrections obtained from anharmonic force fields that have been applied to experimental GED distances (r_a) caused the shortening of the B–N distances (for $r_{a3,1}$) when compared to those of the r_{h1}-type[54] SARACEN[22] refinements that utilised curvilinear corrections. All the compounds adopted different arrangements in the solid phase at 90 K. For instance, methylamine-borane exists in the orthorhombic form like AB, while dimethyl and trimethyl amine boranes assume monoclinic and rhombohedral arrangements. Similar to AB, the methyl and dimethyl complexes showed a significant dihydrogen bond interaction with a

distance of ~200 pm. It is evident from Table 1 that increasing methyl substitution on the N atom increases the B–N distance which may also lead to a decrease in the stability of the bond. However, the predicted B–N bond dissociation energy ($B–N_{BDE}$) provided in Table 1 has indicated a contrary situation regarding the stability in mono and dimethylamine boranes. This may be because there is a decrease in the number of the dihydrogen bonds that are formed with increase in the methyl substitution. Dihydrogen bonds have been shown to induce stability in donor-acceptor complexes.[55] Therefore, it is reasonable to suggest that the stability is linked to the $B–N_{BDE}$ (and by extension to the dihydrogen bonds) more than to the length of the B–N bond.

Another XRD structure determination for methylamine borane also obtained the same orthorhombic structure [*r*B–N = 158.7(3) pm] but, at 298 K, the complex crystallises in a tetragonal lattice with a B–N distance of 159.7(3) pm.[56] The B–N bond distances are similar to those found in AB previously.[49] An initial MWS study on the expected less stable trimethyl amine borane[57] obtained an inaccurate structure due to the inability to locate the ^{15}N isotope as the N lies closer to the centre of mass and also because of the substantial vibration-rotation effects. To circumvent the above issues, Pierce's double substitution approach[58] was used to obtain a more reliable structure [r_sB–N = 163.8(1) pm].[59] However, the Pierce method failed again to locate the position of the N atom. A combination of GED and the rotational constants from MWS suggested a more reliable structure [r_gB–N = 165.6(2) pm].[60] This was achieved after studying a series of closely related halo-substituted ABs[61-63] shown in Table 2 by GED, or a combination of GED and MWS in some cases. Compared to the free amines and BX_3 (X = F, Cl, Br or I), the structural changes are more pronounced in the acceptor parts while changes in the parameters increase with the size of the halogen atom which then agrees with the reorganisation energies of BX_3. Apart from the B–N internuclear distance, all the molecular parameters in $Me_3N–BF_3$ are similar to those in Me_3NBH_3. This suggests the similarity of the acceptor power of BF_3 and BH_3 based on the measured enthalpy change.[64] Although the dative distance in these types of complexes depends on the size of the halogen, it is surprising that the distance in $Me_3N–BF_3$ decreased compared to the others while those in the bromine and iodine analogues are similar. This may be due to the rotational constants that have been employed in the structural analysis of the former which have not been used for the other complexes. While it is a known fact that different weighting schemes may produce different results for the structural parameters, it is surprising that these results for the trimethylamine series agree more with the MWS value of Bryan and Kuczkowski[65] [r_oB–N = 163.6(4) pm]. The single crystal data shown in Table 2 showing a marked shrinkage in the B–N distances from chlorine to the iodine complex is consistent with the dipole moment studies based on the acceptor power of trihalides to form a complex with trimethylamine.[66, 67]

Table 1. B-N internuclear distances[a] of methyl-substituted ABs using different structure determination methods[53] and the experimental $B–N_{BDEs}$ of the respective B-N bonds.

Molecule	$r_{a3,1}$	r_{h1}	XRD	$B–N_{BDE}$[b]
$MeH_2N.BH_3$	160.2(7)	163.3(7)	159.4(13)	146.4(8)
$Me_2HN.BH_3$	161.5(4)	164.2(4)	159.7(13)	152.3(10)
$Me_3N.BH_3$	162.3(2)	165.2(2)	161.7(4)	145.6(5)

[a] Units in pm. Figures in parentheses are the estimated standard deviation of the last digits expressed as 2σ.

[b] Units in kJ/mol, experimental values from reference 17

When the three hydrogens on the boron atom are replaced with electron donating and bulky methyl groups, the structural rearrangement caused the elongation of the B–N bond in both the solid and gas-phase. For instance, the single crystal structure reported for $Me_2HN–BMe_3$[68] has the longest B–N distance [*r*B–N = 165.6(4) pm] ever reported in the solid phase for linear AB systems. A similar result was obtained for $Me_3N–BMe_3$ [r_sB–N = 169.8(1) pm][69] in the gas phase using MWS. $Me_3N–BMe_3$ is less stable than $Me_3N–BF_3$ which is likely due to the former having lower B–N bond dissociation energy as a result of the reorganisation energy of BF_3 being lower than BMe_3 (73.6 *vs* 111.3 kJ/mol). Therefore, the reorganisation energy of the acids plays a role in determining the stabilities of D–A complexes.

Table 2. B-N bond lengths of halo-substituted ABs using different structure determination methods. Distances in pm.

Molecule	r_g	r_a	XRD
$Me_3N.BF_3$	167.4(4)[61]	166.4(1)[15]	158.5(30)[70]
$Me_3N.BCl_3$	165.2(9)[62]	165.9(6)[15]	160.9(6)[71]
$Me_3N.BBr_3$	166.3(13)[62]	-	160.0(2)[71]
$Me_3N.BI_3$	166.3(13)[63]	-	158.0(3)[71]

N-H-containing heterocyclic D-A complexes

N-H containing heterocyclic D-A complexes are ring-containing secondary amine boranes having an $N–BH_3$ unit(s). The first in this series is aziridine borane which was characterised by Ringertz as early as 1969 using XRD.[72] The study yielded an orthorhombic structure with a *Pmnb* space group having a B–N internuclear distance of 155.8(6) pm. A spectroscopic (IR and NMR) study carried out by Williams[73] corroborated Ringertz's observations. In the gas-phase, MWS augmented by QC was used to determine its structure[74] resulting in a complex with C_s symmetry connecting the bisector of the aziridine ring similar to the XRD structure, with the B–N bond having a distance of 161.5 pm. This distance is the approximation to the equilibrium bond length obtained at the MP2/aug-cc-pVTZ level of theory. While MWS was used to determine the dipole moment and barrier to internal rotation, the study relied on the *ab initio* calculations to determine the B–N distance. Recently, we have attempted to determine the structure of azetidine borane using GED. However, only its dehydrogenated form was interrogated in the electron beam.[75] This was followed by a succession of structural studies of larger ring but related complexes,

namely; borane complexes of pyrrolidine,[76] piperidine[76] and morpholine[77] as well as 1,4-bis(borane)piperazine.[78]

Table 3. B-N internuclear distances[a] of N-H-containing heterocyclic D-A complexes obtained using GED and XRD techniques

Molecule	r_{h1}	XRD	B–N_{BDE} [b]
aziridine borane	161.5[c]	155.8(6)	141.0[d]
azetidine borane	162.4[e]	–	161.2
pyrrolidine borane	162.8(5)	–	179.6
piperidine borane	163.9(5)	–	189.6
morpholine borane	164.4(6)	160.5(9)	180.3
1,4–bis(borane) piperazine	163.2(6)	160.1(2)	170.3, 182.0

[a] Units in pm. Figures in parentheses are the estimated standard deviation of the last digits expressed as 2σ.

[b] Units in kJ/mol, values calculated at CCSD(T)/CBS level of theory. For 1,4-bis(borane)piperazine, the two B-N_{BDE} correspond to the BDE of the first and second B-N bonds.

[c] Value calculated at MP2/aug-cc-pVTZ level of theory[74]

[d] Value calculated at G4(MP2) level of theory[79]

[e] Value calculated at MP2/6-311+G* level of theory[75]

The experimentally determined structures are in good agreement with the calculated structures as well as those reported in the literature for similar compounds. Small variations in the bond distances and angles of the complexes have been observed in comparison to their corresponding free cyclic amines. Significant differences between the structures in the gas phase and solid state for morpholine borane and 1,4-bis(borane)piperazine have not been observed except the length of the important B–N interaction. The B–N internuclear distance was found to be shorter in the solid state due to the effects of crystal packing and dipole moments and also because of the nature of what is being measured in the experiments; electron density distribution in the solid state and internclear distance in the gas phase. The B–N distance was also found to increase with ring size from azetidine borane to piperidine borane, a trend also seen in linear amine boranes. The B–N internuclear distances obtained using the various methods previously mentioned are summarised in Table 3. From the B–N_{BDE} values calculated at CCSD(T)/CBS level, it can be said that the stability of the B–N bond increases from azetidine borane to piperidine borane and then decreases towards 1,4-bis(borane) piperazine. This trend, however, is contrary to the lengths of the corresponding B–N bonds since it is believed that shorter bonds are stronger than longer ones. This situation may be peculiar to amine boranes since the same scenario was observed in linear amine boranes as discussed above.[17, 53]

Conclusions

The B–N interaction in various donor-acceptor complexes including cyclic amine boranes characterised using different structural methods have been reviewed. The lengthening of the B–N bond in the gas phase relative to the solid state was observed; a trend consistent with established phenomena. The increase in the dipole moment of structures determined in the gas phase to the solid state allowed the intermolecular forces in the crystal to supply the energy incentive needed to contract the bonds. The stability of the B–N bond in the D–A complexes depends on the number of the dihydrogen bonds that are likely to be formed rather than the lengths of the B–N bond. This assertion has been supported by the B–N_{BDEs} determined experimentally for the linear complexes as well as the predicted values obtained from accurate thermochemical methods.

References

1. Lewis, G. N. *J. Franklin I.* **1938,** *226* (3), 293-313.
2. Abboud, J. L. M.; Németh, B.; Guillemin, J. C.; Burk, P.; Adamson, A.; Nerut, E. R. *Chem. Eur. J.* **2012,** *18* (13), 3981-3991.
3. Staubitz, A.; Robertson, A. P. M.; Sloan, M. E.; Manners, I. *Chem. Rev.* **2010,** *110* (7), 4023-4078.
4. Bluhm, M. E.; Bradley, M. G.; Butterick, R.; Kusari, U.; Sneddon, L. G. *J. Am. Chem. Soc.* **2006,** *128* (24), 7748-7749.
5. Tarozaitė, R.; Sudavičius, A.; Sukackienė, Z.; Norkus, E. *Int. J. Surf. Eng. Coatings* **2014,** *92* (3), 146-152.
6. Sukackienė, Z.; Tamašauskaitė-Tamašiūnaitė, L.; Jasulaitienė, V.; Balčiūnaitė, A.; Naujokaitis, A.; Norkus, E. *Thin Solid Films* **2017,** *636*, 425-430.
7. Ramachandran, P. V.; Kulkarni, A. S.; Zhao, Y.; Mei, J. *Chem. Comm.* **2016,** *52* (80), 11885-11888.
8. White, S. S.; Kelly, H. C. *J. Am. Chem. Soc.* **1968,** *90* (8), 2009-2011.
9. White Jr, S. S.; Kelly, H. C. *J. Am. Chem. Soc.* **1970,** *92* (14), 4203-4209.
10. Wolfe, T. C.; Kelly, H. C. *J. Chem. Soc. Perkin Trans. 2* **1973,** (14), 1948-1950.
11. Wilson, I.; Kelly, H. C. *Inorg. Chem.* **1982,** *21* (4), 1622-1627.
12. Smith, W. B. *J. Org. Chem.* **1984,** *49* (17), 3219-3220.
13. Sakai, S. *J. Phys. Chem.* **1995,** *99* (22), 9080-9086.
14. Anane, H.; Jarid, A.; Boutalib, A.; Nebot-Gil, I.; Tomás, F. *J. Mol. Struct.: THEOCHEM* **1998,** *455* (1), 51-57.
15. Hargittai, M.; Hargittai, I. *J. Mol. Struct.* **1977,** *39* (1), 79-89.
16. Bader, R. F.; Gillespie, R. J.; MacDougall, P. J. *J. Am. Chem. Soc.* **1988,** *110* (22), 7329-7336.
17. Haaland, A. *Angew. Chem. Int. Ed.* **1989,** *28* (8), 992-1007.
18. Jagielska, A.; Moszyński, R.; Piela, L. *J. Chem. Phys.* **1999,** *110* (2), 947-954.
19. Klimkowski, V.; Ewbank, J.; Van Alsenoy, C.; Scarsdale, J.; Schaefer, L. *J. Am. Chem. Soc.* **1982,** *104* (6), 1476-1480.
20. Blake, A. J.; Brain, P. T.; McNab, H.; Miller, J.; Morrison, C. A.; Parsons, S.; Rankin, D. W. H.; Robertson, H. E.; Smart, B. A. *J. Phys. Chem.* **1996,** *100* (30), 12280-12287.
21. Brain, P. T.; Morrison, C. A.; Parsons, S.; Rankin, D. W. H. *Dalton Trans.* **1996,** (24), 4589-4596.
22. Mitzel, N. W.; Rankin, D. W. H. *Dalton Trans.* **2003,** (19), 3650-3662.
23. Staubitz, A.; Robertson, A. P.; Manners, I. *Chem. Rev.* **2010,** *110* (7), 4079-4124.
24. Richardson, T.; de Gala, S.; Crabtree, R. H.; Siegbahn, P. E. *J. Am. Chem. Soc.* **1995,** *117* (51), 12875-12876.
25. Hu, M.; Geanangel, R.; Wendlandt, W. *Thermochim. Acta* **1978,** *23* (2), 249-255.
26. Grant, D. J.; Matus, M. H.; Anderson, K. D.; Camaioni, D. M.; Neufeldt, S. R.; Lane, C. F.; Dixon, D. A. *J. Phys. Chem. A.* **2009,** *113* (21), 6121-6132.

27. Becerra, M.; Real-Enriquez, M.; Espinosa-Gavilanes, C.; Zambrano, C. H.; Almeida, R.; Torres, F. J.; Rincón, L. *Theo. Chem. Acc.* **2016,** *135* (3), 1-11.
28. Sim, G. A.; Sutton, L. E. In *Molecular structure by diffraction methods*, Chemical Society: London, 1972, 17-18.
29. Ebsworth, E. A. V.; Rankin, D. W. H.; Cradock, S. In *Structural methods in inorganic chemistry*; Blackwell Scientific Publications: Oxford, 1987, 5-6.
30. Hargittai, I.; Hargittai, M. In *Encyclopedia of spectroscopy and spectrometry*, Elsevier, 2010, 461-465.
31. McCaffrey, P. D.; Mawhorter, R. J.; Turner, A. R.; Brain, P. T.; Rankin, D. W. H. *J. Phys. Chem. A.* **2007,** *111* (27), 6103-6114.
32. Hamilton, C. W.; Baker, R. T.; Staubitz, A.; Manners, I. *Chem. Soc. Rev.* **2009,** *38* (1), 279-293.
33. Lane, C. L. **2006**, see: http://www1.eere.energy.gov/hydrogenandfuelcells/pdfs/nbh_h2_storage_survey.pdf (accessed 19/02/20).
34. Hutchins, R. O.; Learn, K.; Nazer, B.; Pytlewski, D.; Pelter, A. *Org. Prep. Proced. Int*. **1984,** *16* (5), 335-372.
35. Stephens, F. H.; Pons, V.; Baker, R. T. *Dalton Trans.* **2007,** (25), 2613-2626.
36. Umegaki, T.; Yan, J.-M.; Zhang, X.-B.; Shioyama, H.; Kuriyama, N.; Xu, Q. *Int. J. Hydrogen Energy* **2009,** *34* (5), 2303-2311.
37. Fakioğlu, E.; Yürüm, Y.; Veziroğlu, T. N. *Int. J. Hydrogen Energy* **2004,** *29* (13), 1371-1376.
38. Shore, S. G.; Parry, R. W. *J. Am. Chem. Soc.* **1955,** *77* (22), 6084-6085.
39. Weaver, J.; Shore, S. G.; Parry, R. *J. Chem. Phys.* **1958,** *29* (1), 1-2.
40. Suenram, R.; Thorne, L. *Chem. Phys. Lett.* **1981,** *78* (1), 157-160.
41. Hughes, E. W. *J. Am. Chem. Soc.* **1956,** *78* (2), 502-503.
42. Lippert, E. L.; Lipscomb, W. N. *J. Am. Chem. Soc.* **1956,** *78* (2), 503-504.
43. Sorokin, V. P.; Vesnina, B. V.; Klimova, N. S. *J. Inorg. Chem* **1963,** *8* (1), 32.
44. Hoon, C.; Reynhardt, E. *J. Phys. C.: Sol. Stat. Phys.* **1983,** *16* (32), 6129.
45. Wang, L.; Duan, D.; Zhao, B.; Bao, K.; Yu, H. *J. Phys. Chem. C* **2019,** *123* (11), 6326-6332.
46. Bühl, M.; Steinke, T.; von Ragué Schleyer, P.; Boese, R. *Angew. Chem. Int. Ed.* **1991,** *30* (9), 1160-1161.
47. Montgomery Jr, J. A.; Frisch, M. J.; Ochterski, J. W.; Petersson, G. A. *J. Chem. Phys.* **2000,** *112* (15), 6532-6542.
48. Klooster, W. T.; Koetzle, T. F.; Siegbahn, P. E. M.; Richardson, T. B.; Crabtree, R. H. *J. Am. Chem. Soc.* **1999,** *121* (27), 6337-6343.
49. Bowden, M. E.; Gainsford, G. J.; Robinson, W. T. *Aust. J. Chem.* **2007,** *60* (3), 149-153.
50. Thorne, L.; Suenram, R.; Lovas, F. *J. Chem. Phys.* **1983,** *78* (1), 167-171.
51. Hargittai, M.; Hargittai, I. *Phys. Chem. Min.* **1987,** *14* (5), 413-425.
52. Demaison, J.; Liévin, J.; Császár, A. G.; Gutle, C. *J. Phys. Chem. A.* **2008,** *112* (19), 4477-4482.
53. Aldridge, S.; Downs, A. J.; Tang, C. Y.; Parsons, S.; Clarke, M. C.; Johnstone, R. D. L.; Robertson, H. E.; Rankin, D. W. H.; Wann, D. A. *J. Am. Chem. Soc.* **2009,** *131* (6), 2231-2243.
54. Wann, D. A.; Less, R. J.; Rataboul, F.; McCaffrey, P. D.; Reilly, A. M.; Robertson, H. E.; Lickiss, P. D.; Rankin, D. W. H. *Organomet.* **2008,** *27* (16), 4183-4187.
55. Popelier, P. L. A. *J. Phys. Chem. A.* **1998,** *102* (10), 1873-1878.
56. Bowden, M. E.; Brown, I. W.; Gainsford, G. J.; Wong, H. *Inorg. Chim. Acta* **2008,** *361* (7), 2147-2153.
57. Durig, J. R.; Li, Y. S.; Odom, J. D. *J. Mol. Struct.* **1973,** *16* (3), 443-450.
58. Pierce, L. *J. Mol. Spectrosc.* **1959,** *3* (1), 575-580.
59. Cassoux, P.; Kuczkowski, R. L.; Bryan, P. S.; Taylor, R. C. *Inorg. Chem.* **1975,** *14* (1), 126-129.
60. Iijima, K.; Adachi, N.; Shibata, S. *Bull. Chem. Soc. Jpn.* **1984,** *57* (11), 3269-3273.
61. Iijima, K.; Shibata, S. *Bull. Chem. Soc. Jpn.* **1979,** *52* (3), 711-715.
62. Iijima, K.; Shibata, S. *Bull. Chem. Soc. Jpn.* **1980,** *53* (7), 1908-1913.
63. Iijima, K.; Shibata, S. *Bull. Chem. Soc. Jpn.* **1983,** *56* (7), 1891-1895.
64. Brown, H. C.; Holmes, R. R. *J. Am. Chem. Soc.* **1956,** *78* (10), 2173-2176.
65. Kuczkowski, R. L.; Bryan, P. S. *Inorg. Chem.* **1971,** *10* (1), 200-201.
66. Bax, C. M.; Katritzky, A. R.; Sutton, L. E. *J. Chem. Soc* **1958,** *1258*.
67. Miller, J. M.; Onyszchuk, M. *Can. J. Chem.* **1963,** *41* (11), 2898-2902.
68. Ouzounis, K.; Riffel, H.; Hess, H. *J. Organomet. Chem.* **1987,** *332* (3), 253-258.
69. Kuznesof, P. M.; Kuczkowski, R. L. *Inorg. Chem.* **1978,** *17* (8), 2308-2311.
70. Geller, S.; Hoard, J. L. *Acta Crystallogr.* **1951,** *4*, 399.
71. Clippard, P. H.; Hanson, J. C.; Taylor, R. C. *J. Cryst. Mol. Struct.* **1971,** *1* (6), 363-371.
72. Ringertz, H. *Acta Chem. Scand.* **1969,** *23* (1), 137443.
73. Williams, R. *Acta Chem. Scand.* **1969,** *23* (1), 149.
74. Konovalov, A.; Møllendal, H.; Guillemin, J.-C. *J. Phys. Chem. A.* **2009,** *113* (29), 8337-8342.
75. Ja'o, A. M.; Masters, S. L.; Wann, D. A.; Rankine, C. D.; Nunes, J. P. F.; Guillemin, J.-C. *J. Phys. Chem. A.* **2019,** *123* (32), 7104-7112.
76. Ja'o, A. M.; Masters, S. L.; Wann, D. A.; Rankine, C. D.; Nunes, J. P. F.; Guillemin, J.-C. *Manuscript in preparation*.
77. Ja'o, A.; Wann, D.; Rankine, C.; Polson, M.; Masters, S. *Aust. J. Chem.* **2020,** *Accepted 25 November 2019*.
78. Ja'o, A. M.; Masters, S. L.; Wann, D. A.; Rankine, C. D.; Benetis, J.; Polson, M. I. J. *Manuscript in preparation*.
79. Banu, T.; Sen, K.; Ghosh, D.; Debnath, T.; Das, A. K. *RSC Adv.* **2014,** *4* (3), 1352-1361.

Article

Studies towards the fast and efficient synthesis of LL-Z1640-2: synthesis of the complete LL-Z1640-2 framework

Suzannah J. Harnor,[1] Murray N. Robertson,[1] Neil Henry,[1] Zachariah Stueven,[2] Rodolfo Marquez[1,2*] (email: *rudi.marquez@canterbury.ac.nz*)

[1]School of Chemistry, University of Glasgow, Glasgow G12 8QQ

[2]School of Physical and Chemical Sciences, University of Canterbury, Christchurch 8140

Keywords: *LL-Z1640-2, synthesis, resorcyclic lactones*

Dedicated to the loving memory of Lilly Rose Taylor, R.I.P.

LL-Z1640-2 (also known as 5*Z*-7-Oxo-zeaenol and C292) **1** was isolated in 1978 from the culture broth of fungal strain f6024. Although it was originally classified as an anti-protozoan agent, it was not until 1999 that its cytokine release inhibiting activity was discovered. LL-Z1640-2 has been shown to be a selective protein tyrosine kinase inhibitor, not inhibiting either PKA or PKC. Preliminary data also suggests that LL-Z1640-2 is selective amongst a variety of protein tyrosine kinases.,

LL-Z1640-2 **1** is structurally related to 14 membered macrocyclic lactones hypothemycin **2**, 87-250904-F1 **3**, 7-oxo-zeaenol **4**, zeaenol **5**, radicicol **6**, and various simpler zearalanone and zearalanols. Furthermore, 87-250904-F1 **3** and radicicol **6** have been shown to be specific inhibitors of the expression of COX-2, an enzyme responsible for the synthesis of the proinflammatory mediators, prostaglandins.

It is based on this set of remarkable biological activities, together with their interesting structural features, that has prompted us to consider a flexible synthesis of LL-Z1640-2 **1**. Although there has been a significant amount of interest in the syntheses of resorcyclic lactones, particularly radicicol **6** and the pochonins, the efforts towards LL-Z1640-2 **1** have been somewhat limited.-11

Herein we present our efforts towards a flexible and robust synthesis of LL-Z1640-2 **1** beginning from readily available starting materials. Retrosynthetically, LL-Z1640-2 **1** was envisioned as originating from the macrolactonisation of the corresponding seco-acid **7** which in turn originates from the cross metathesis reaction of the aryl alkene **8** and the complete C_1-C_{11} alkene **9** (Scheme 1).

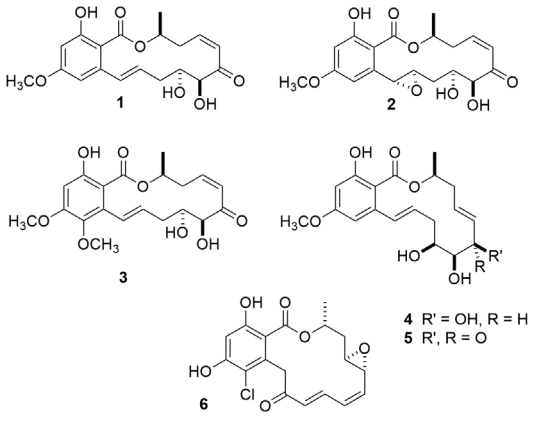

Scheme 1. Retrosynthetic analysis of LL-Z1640-2, **1**

Alkene **9** on the other hand, was thought as having originated from alkynol **10**, which could have been produced by the addition of alkyne **12** to aldehyde **11**. Aldehyde **11** is the direct product of the Wittig olefination of 2-deoxy-ribose **13**.

Our synthesis began with 2,4,6-trihydroxybenzoate **14** which, after selective methylation at the 4-position, afforded diphenol **15,** which was then mono-protected to generate silyl ether **16**. Conversion of the remaining hydroxyl group into the corresponding triflate **17** proceeded under carefully controlled conditions.[12] The triflate was then subjected to Stille coupling conditions with vinyltributyltin to generate the desired alkene **18** together with phenol **19**.[13] Treatment of the mixture of esters **18** and **19** with TBAF proceeded to generate the aromatic fragment **20** in 74% yield over two steps (Scheme 2).

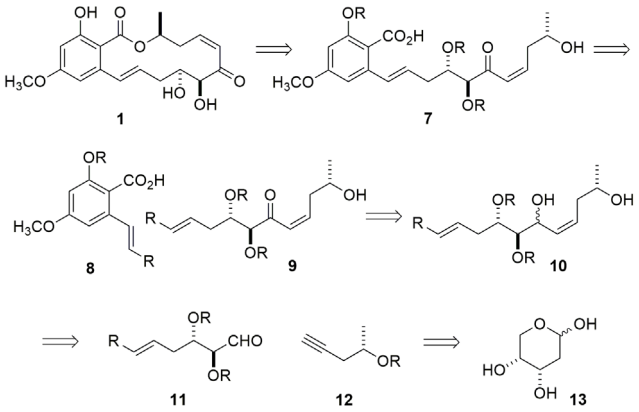

Scheme 2. Synthesis of aromatic fragment **20**. *Reagents and Conditions:* (a) TMS-CH_2N_2, Et_2O, 0ºC, 15h; 90%; (b) TBDMSCl, Et_3N, CH_2Cl_2, rt, 20h; 80%; (c) Tf_2O, pyridine, DMF, 0ºC, 3h; 100%: (d) vinyltributyltin, $Pd(PPh_3)_4$, DMF, 60ºC, 3h; (e) TBAF, THF, 0° C -> rt, 2h; 74% (*over 2 steps*).

The synthesis of linear alkene unit **9** began with 2-deoxy-D-ribose **13** which was protected as ketal **21** (Scheme 3).[14] Wittig olefination of lactol **21** using methyltriphenylphosphonium iodide then proceeded to afford **22** with the desired terminal alkene in acceptable yield.[15] Protection of the primary alcohol as the TBS silyl ether proceeded in good yield to give the desired alkene cross-metathesis coupling partner **23**.

Having successfully obtained both alkene partners, the key cross-coupling reaction was attempted. Gratifyingly, using 30 mol% loading of Hoveyda-Grubgs II catalyst and a 2:1 ratio of alkenes **23** to **20**, the desired product **24** was obtained in good yield and as a 9:1 (*E:Z*) ration of isomers (Scheme 4).

Protection of the free phenolic group then afforded the desired MOM ether **25**. Treatment of ether **25** with TBAF then generated the desired free alcohol **26** in good yield over both steps (Scheme 5).

The synthesis of the *seco*-acid epimer **12** began with lithium acetylide ethylenediamine, which was treated with *(R)*-(+)-propylene oxide **22** to afford the crude alcohol **28** (Scheme 6). Alcohol **28** was then immediately protected as the PMB ether to generate the key terminal alkyne **29** in 40% over two steps.

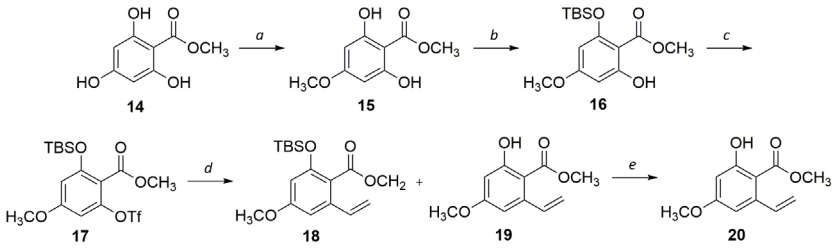

Scheme 3. Synthesis of Alkene **23.** Reagents and Conditions: (a) 2-Methoxypropene, PPTS, EtOAc, -10 °C, 2.5 h *then* rt, 16 h, 62%; (b) $(Ph_3P\text{-}CH_3)I$, KHMDS, THF, -78 °C -> rt, 17 h, 60%; (c) TBDMSCl, DMAP, Et_3N, CH_2Cl_2, rt, 18 h, 87%.

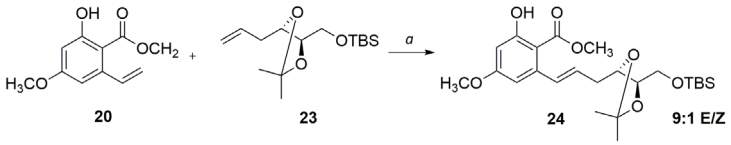

Scheme 4. Cross-metathesis of alkenes **20** and **23**. *Reagents and Conditions:* (a) Hoveyda-Grubbs second generation catalyst (30 mol%), CH_2Cl_2, reflux, 48 h, 65%.

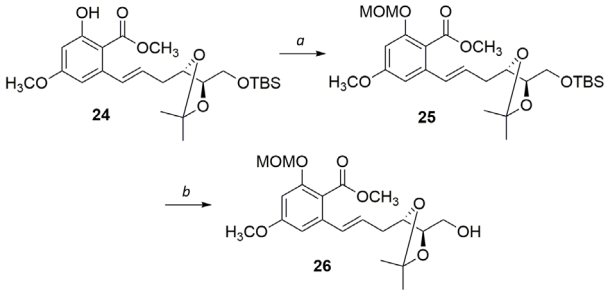

Scheme 5. Synthesis of primary alcohol **26**. *Reagents and Conditions*: (a) MOMBr, DIPEA, CH_2Cl_2, 0 °C -> rt, 18 h, 60%; (b) TBAF, THF, 0 °C -> rt, 1.5, 93%.

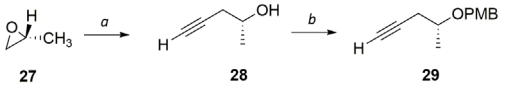

Scheme 6. Synthesis of terminal olefin **29**. *Reagents and Conditions*: (a) lithium acetylide ethylenediamine complex, DMSO, 0 °C -> rt, 48 h; (b) NaH (60% in mineral oil), PMBCl, DMF, 0 °C -> rt, 17 h, 40% (*over 2 steps*).

The remaining steps of the synthesis began with alkyne **29**, which was deprotonated with ethylmagnesium bromide, and the resulting anion was added directly to a solution of freshly generated aldehyde (**26→30**) at —78 °C. Pleasingly, the Grignard acetylide added cleanly to the aldehyde, affording propargylic alcohol **31** in good yield, albeit as an inseparable mixture of diastereoisomers (Scheme 7). Protection of alcohol **31** as the TIPS silyl ether **32**, followed by selective hydrogenation generated the desired *Z*-olefin **33** in excellent yield. Oxidative removal of the PMB group with DDQ afforded the desired secondary alcohol **34** in good yield. Saponification of methyl ester **34** with potassium hydroxide proceeded to afford the key *seco*acid intermediate **35** in acceptable yield.

Gratifyingly, the key Mitsunobu macrolactonisation of *seco*-acid **35** proceeded to generate the key macrocyclic lactone **36** in 73% yield. Selective TIPS removal produced alcohol **37**, which upon PPC oxidation generated the desired lactone **38** in 34% yield.

In conclusion, we have completed the synthesis of the complete LL-Z1640-2 **1** framework. The synthesis developed is convergent and amenable for the generation of new analogues.

Experimental

All reactions were performed under an inert argon atmosphere unless otherwise noted. Reagents and starting materials were obtained from commercial sources and used as received, unless otherwise specified. Anhydrous dichloromethane (DCM), diethyl ether, toluene and tetrahydrofuran (THF) were freshly obtained from an in-house solvent purification system, Pure Solv 400-5MD (Innovative Technology, Inc). Anhydrous dimethylformamide (DMF) and triethylamine (TEA) were purchased from Aldrich Chemical Company. Petroleum ether refers to that with boiling fraction 40—60 °C. Solutions worked up were concentrated under reduced pressure at < 45 °C using a Buchi Rotavapor. Melting points were determined using Stuart Scientific Melting Point SMP1 apparatus.

Optical rotations were determined as solutions irradiating with the sodium D line (λ = 598 nm) using an AA series automatic polarimeter. $[\alpha]_D$ values are given in units 10^{-1} deg cm^2 g^{-1}. Infrared (IR) spectra were recorded as thin films on sodium chloride (NaCl) plates using a JASCO FTIR 410 spectrometer. Only significant absorptions (ν_{max}) are reported in wavenumbers (cm^{-1}). Proton magnetic resonance spectra (^{1}H NMR) were recorded at 400 MHz using a Bruker DPX-400 spectrometer for sample solutions in $CDCl_3$, unless otherwise indicated. Chemical shifts (δH) are reported in parts per million (ppm) and are referenced to the residual solvent peak. The order of citation in parentheses is (1) number of equivalent nuclei (by integration) (2) multiplicity (s = singlet, d = doublet, t = triplet, q = quartet, qn = quintet, sext. = sextet, oct. = octet, m = multiplet, br = broad) (3) and coupling constant (*J*) quoted in Hertz to the nearest 0.1 Hz. For relevant compounds, the OH signal was identified by D_2O exchange.

Carbon magnetic resonance spectra (^{13}C NMR) were recorded at 100 MHz using a Bruker DPX-400 spectrometer for sample solutions in $CDCl_3$, unless otherwise indicated. Chemical shifts (δC) are quoted in parts per million (ppm) and are referenced to the residual solvent peak. Mass spectra were obtained using a JEOL JMS-700 spectrometer. TLC was performed on aluminium backed plates pre-coated with silica gel 60 (Kieselgel 60 F254 aluminium plates, Merck) and detection under UV light (λmax 254 nm) and/or by staining with anisaldehyde, unless otherwise specified, followed by heating.

Flash column chromatography (FCC) was performed using Apollo Scientific silica gel 60 (0.040-0.063 mm), with the appropriate eluting solvent and elution gradient, shown in square brackets as part of the procedure.

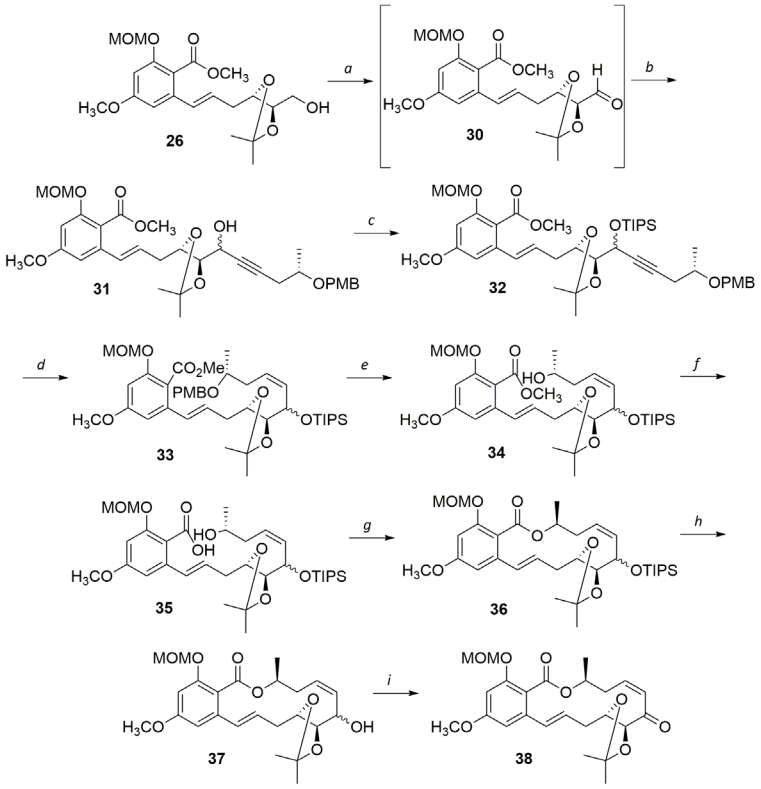

Scheme 7. Synthesis of the complete LL-Z1640-2 framework. *Reagents and Conditions:* (a) $(COCl)_2$, DMSO, Et_3N, -78 °C -> rt; (b) **29**, THF, -78 °C -> rt, 16 h, 75%; (c) TIPSCl, imidazole, DMF, rt, 19 h, 80%; (d) H_2, $Pd/BaSO_4$, quinoline, MeOH, rt, 2h, 89%; (e) DDQ, CH_2Cl_2, pH 7 buffer, rt, 18 h, 87%; (f) 2N KOH, EtOH, 80 °C, 48 h, 61%; (g) DEAD, PPh_3, toluene, 0 °C -> rt, 10 min, 73%; (h) TBAF, THF, 0 °C -> rt, 1 h; (i) PCC, CH_2Cl_2, rt, 18 h, 34%.

2-Deoxy-3,4-*O*-isopropylidene-D-pentopyranose, 21

Under an argon atmosphere, a -10°C stirred solution of 2-deoxy-D-ribose **13** (3.0 g,22.4 mmol) in ethyl acetate (150 mL) was treated with 2-methoxypropene (2.8 mL, 29.1 mmol) and pyridinium *p*-toluenesulfonate (224 mg, 0.694 mmol). The solution was allowed to stir at -10°C for 2.5 h before allowing it to warm up to room temperature overnight. The reaction was quenched with triethylamine (1.5 mL, 10.8 mmol) and then concentrated *in vacuo*. Purification by FCC [petroleum ether-ethyl acetate (90 :10)→(80:20)→(70:30)→(50:50)] of the crude residue afforded ketal **21** (2.39 g, 62%) as a white solid.

$[\alpha]^{20}_{D}$ –29.3 (*c* 1.1, $CHCl_3$) (lit.,[51] $[\alpha]^{21}_{D}$ –46.0 (*c* 0.1, water); *v*max(film)/cm^{-1} 2984, 2938,1663, 1369; ^{1}H NMR (400 MHz; $CDCl_3$) (major α anomer) δ 1.31 (3 H, s),1.48 (3 H, s), 1.75 (1H, ddd, *J* = 14.8, 7.0, 4.2 Hz), 2.22 (1H, dt, *J* = 14.8, 4.2 Hz), 3.67 (1H, dd, *J* = 12.7, 3.6 Hz), 3.94 (1H, dd, *J* = 12.7, 3.6 Hz), 4.12-4.16 (1H, m), 4.41-4.47 (1H, m), 5.23 (1H,dd, *J* = 7.2, 4.2 Hz); ^{13}C (100 MHz;CDCl3) δ 108.8, 90.9, 71.6, 70.8, 62.1, 32.1, 27.3, 25.4; MS (EI) *m/z* 197 $[M]^+$; HRMS *m/z* 197.0772 (197.0784 calcd for $C_8H_{14}NaO_4$, M^+); ^{1}H NMR (400 MHz; $CDCl_3$) (minor β anomer) δ 1.32 (3H, s), 1.57 (3H, s), 2.10 (2H, t, *J* = 3.8 Hz), 3.65-3.71 (1H, m), 3.95-4.02 (1H, m), 4.13-4.23 (1H, m), 4.43-4.45 (1H, m) and 5.09 (1H, m). All spectral data matches that reported in the literature.[14]

((4*S*,5*R*)-5-Allyl-2,2-dimethyl-[1,3]dioxolan-4-yl)-methanol, 22

Potassium bis(trimethylsilyl)amide (32 mL, 16.1 mmol) was added to a -78°C stirred suspension of methyl triphenylphosphonium iodide (8.74 g, 21.5 mmol) in anhydrous tetrahydrofuran (40 mL). The reaction was warmed up to 0°C and stirred for 30 min before cooling back down to -78°C. A solution of acetonide **21** (937 g, 5.38 mmol) in anhydrous tetrahydrofuran (10 mL) was added, and the yellow solution was warmed up to room temperature overnight. The reaction was quenched with saturated aqueous ammonium chloride (50 mL) and extracted with ethyl acetate (3x50 mL). The organic layers were combined, dried over anhydrous sodium sulfate, filtered and concentrated *in vacuo*. Purification by FCC [petroleum ether-ethyl acetate (100:0)→(70:30)→(60:40)] of the crude residue afforded alcohol **22** (557 g, 60%) as a yellow oil.

*v*max (film)/cm^{-1} 3450, 2987, 2853, 1643, 1457, 1379, 1235, 1217, 1045; ^{1}H NMR (400 MHz; $CDCl_3$) δ 1.37 (3H, s), 1.48 (3H, s), 2.23-2.32 (1H, m), 2.36-2.46 (1H, m), 3.64 (2H, t, *J* = 5.8 Hz), 4.17 (1H, q, *J* = 5.9 Hz), 4.25 (1H, q, *J* = 5.9 Hz), 5.09-5.18 (2H, m), 5.78-5.90 (1H, m); ^{13}C NMR (100 MHz; $CDCl_3$) δ 25.4, 28.0, 33.5, 61.3, 76.2, 77.8, 108.1, 117.2, 134.2; MS (CI) *m/z* 173 $[M+H]^+$; HRMS *m/z* 173.1174 (173.1178 calcd for $C_9H_{17}O_3$, $M+H^+$). All spectral data matches that reported in the literature.[15]

((4*S*,5*S*)-5-Allyl-2,2-dimethyl-[1,3]dioxolan-4-ylmethoxy)-*tert*butyldimethylsilane, 23

Alcohol **22** (446 mg, 2.59 mmol) was dissolved in anhydrous dichloromethane (13 mL) and triethylamine (0.65 mL, 4.66 mmol) and dimethylaminopyridine (32 mg, 0.259 mmol) were added sequentially at rt. The reaction mixture was stirred for 5 min and then *tert*-butyldimethylsilyl chloride (507 mg, 3.37 mmol) was added. After 18 h, the reaction was quenched with satd. aq. ammonium chloride (10 mL) and extracted with dichloromethane (3x10 mL). The combined organic layers were dried over anhydrous Na_2SO_4, filtered and concentrated *in vacuo*. Purification by FCC [petroleum ether-ethyl acetate (95:5)] of the crude residue afforded silyl ether **23** (643 mg, 87%) as an orange oil.

$[\alpha]^{23}$ –0.4 (*c* 1.0, $CHCl_3$); *v*max (film)/cm^{-1} 2954, 1643, 1472, 1257; ^{1}H NMR (400 MHz; $CDCl_3$) δ: 0.06 (6H, s), 0.89 (9H, s), 1.34 (3H, s), 1.43 (3H, s), 2.29-2.46 (2H, m), 3.59-3.71 (2H, m), 4.03-4.07 (1H, m), 4.18-4.22 (1H, m), 5.00-5.16 (2H, m), 5.83-5.95 (1H, m); ^{13}C NMR (100 MHz; $CDCl_3$) δ: -5.5, -5.4, 18.3, 25.5, 25.9, 28.1, 33.8, 61.9, 76.7, 77.8, 107.9, 116.8, 135.2; MS (CI) *m/z* 287.1 $[M+H]^+$; HRMS *m/z* 287.2047 (287.2042 calcd for $C_{15}H_{31}O_3Si$,$M+H^+$).

Methyl 2-(*tert*-butyldimethylsilanyloxy)-4-methoxy-6-vinyl-benzoate, 18

Lithium chloride (430 mg, 10.1 mmol) was dissolved in anhydrous dimethylformamide (24 mL) and then tri-2-furylphosphine (125 mg, 0.534 mmol) and tris[dibenzylideneacetone] dipalladium(0) (Pd2(dba)3) (62 mg, 67.5 µmol) were added sequentially at room temperature followed by a solution of triflate **17** (1.5 g, 3.37 mmol) in anhydrous dimethylformamide (10 mL). The resulting reaction mixture was stirred for 30 min before tributylvinyl tin (1.2 mL, 4.05 mmol) was added. The reaction solution was heated to 60°C for 3h after which it was cooled back down to rt, diluted with dichloromethane (40 mL) and water (40 mL). The aqueous layer was removed, and the organic phase washed with 1M potassium fluoride aq soln (3x50 mL). The reaction mixture was shaken in a separatory funnel for 1 min for each wash. After the first wash solid tributyltin-fluoride precipitate formed at the interface, and was filtered out through Celite®. The combined organic layers were washed with brine (50 mL), dried over anhydrous Na_2SO_4, filtered and concentrated *in vacuo*. Purification by FCC [petroleum ether-ethyl acetate (100:0)→(95:5) *then* petroleum ether-diethyl ether (100:0)→(95:5)] of the crude residue afforded an inseparable mixture of alkenes **18** and **19** as a white solid mixture.

Compound 18: ^{1}H NMR (400 MHz; $CDCl_3$) δ: 0.01 (6H, s), 0.76 (9H, s), 3.82 (3H, s), 3.91 (3H, s), 5.21 (1H, dd, *J* = 10.8, 1.6 Hz), 5.45 (1H, dd, *J* = 17.1, 1.6 Hz), 6.30 (1H, d, *J* = 2.4 Hz), 6.42 (1H, d, *J* = 2.4 Hz), 6.68-6.75 (1H, m); ^{13}C NMR (100 MHz; $CDCl_3$) δ: -4.3, 17.8, 25.8, 52.0, 55.9, 100.3, 103.5, 108.7, 115.9, 138.4, 143.9, 164.3, 165.0, 171.8.

Compound 19: ^{1}H NMR (400 MHz; $CDCl_3$) δ: 3.78 (3H, s), 3.87 (3H, s), 5.18 (1H, dd, *J* = 10.8, 1.5 Hz), 5.42 (1H, dd, *J* = 17.1, 1.5 Hz), 6.36 (1H, d, *J* = 2.6 Hz), 6.46 (1H, d, *J* = 2.6 Hz), 7.23-7.30 (1H, m), 11.61 (1H, s).

Methyl 2-hydroxy-4-methoxy-6-vinylbenzoate, 20

A solution of alkenes **18** and **19** (736 mg, 2.28 mmol) in anhydrous tetrahydrofuran (10 mL) was cooled down to 0°C. Tetrabutylammonium fluoride (1.0M in THF, 4.5 mL, 4.56 mmol) was added, and the ice-water bath was removed after 10 min, whereafter the reaction was allowed to warm up to rt. After 2h, the reaction mixture was diluted with diethyl ether (30 mL) and diluted with water (30 mL). The organic layer was dried over anhydrous Na_2SO_4, filtered and concentrated *in vacuo*. The crude residue was passed through a pad of silica gel which was eluted with 20% diethyl ether in petroleum ether to remove excess TBS. The fractions were concentrated under reduced pressure to afford phenol **20** (517 mg, 74% *over two steps*) as a white solid.

m.p. 78-80 °C (rec. from diethyl ether-petroleum ether) (lit.[16] 75-76 °C); *v*max (film)/cm^{-1} 2925, 2854, 1733, 1648, 1437, 1328, 1257, 1159; ^{1}H NMR (400 MHz; $CDCl_3$) δ: 3.78 (3H, s), 3.87 (3H, s), 5.18 (1H, dd, *J* = 10.8, 1.6 Hz), 5.42 (1H, dd, *J* = 17.1, 1.6 Hz), 6.36 (1H, d, *J* = 2.6 Hz), 6.46 (1H, d, *J* = 2.6 Hz), 7.23-7.33 (1H, m), 11.61 (1H, s); ^{13}C NMR (100 MHz; $CDCl_3$) δ: 52.1, 55.5, 100.3, 103.9, 108.3, 115.8, 138.4, 143.6, 164.3, 165.1, 171.7; MS (EI) *m/z* 208.0 $[M]^+$; HRMS *m/z* 208.0734 (208.0736 calcd for $C_{11}H_{12}O_4$, M^+). All spectral data matches those reported in the literature.[16]

2-{(*E*)-3-[(4*S*,5*S*)-5-(*tert*-butyldimethylsilanyloxymethyl)-2,2-dimethyl-methyl [1,3]dioxolan-4-yl]-propenyl}-6-hydroxy-4-methoxybenzoate, 24

A stirred solution of styrene **20** (966 mg, 4.64 mmol) and alkene **23** (2.66 g,9.28 mmol) in anh dichloromethane (75 mL) was treated with Hoveyda-Grubbs second generation catalyst (872 mg, 1.39 mmol), and the resulting mixture was heated to reflux in the dark for 48 h. The reaction mixture was allowed to cool down to rt and was then filtered through silica gel and concentrated *in vacuo*. Purification by FCC [petroleum ether-ethyl acetate (95:5)→(90:10)] of the crude residue afforded alkene **24** (1.4 g, 65%) as a colourless oil.

$[\alpha]^{23}$ –1.3 (*c* 1.0, $CHCl_3$); *v*max(film)/cm^{-1} 2930, 2856, 1655, 1437, 1327, 1213, 1159, 1097; ^{1}H NMR (400 MHz; $CDCl_3$) δ: 0.00 (6H, s), 0.82 (9H, s), 1.27 (3H, s), 1.37 (3H, s), 2.35-2.50 (2H, m), 3.55-3.69 (2H, m), 3.80 (3H, s),3.89 (3H, s), 4.12-4.30 (2H, m), 5.98 (1H, dt, *J* = 15.5, 6.9 Hz), 6.36 (1H, d, *J* = 2.5 Hz), 6.48 (1H, d, *J* = 2.5 Hz), 7.01 (1H, d, *J* = 15.5 Hz), 11.61 (1H, s); ^{13}C NMR (100 MHz; $CDCl_3$) δ: -5.3, -5.2, 18.4, 25.7, 26.0, 28.3, 33.2, 52.1, 55.5, 62.0, 77.3, 77.8, 99.9, 103.8, 108.1, 116.6, 129.2, 133.0, 143.2, 164.1, 165.1, 171.9; MS (CI) *m/z* 467 $[M+H]^+$; HRMS *m/z* 467.2466 (467.2465 calcd for $C_{24}H_{39}O_7Si$, $M+H^+$).

Methyl 2-{(*E*)-3-[(4*S*,5*S*)-5-(*tert*-butyldimethylsilanyloxymethyl)-2,2-dimethyl [1,3]dioxolan-4-yl]-propenyl}-4-methoxy-6-methoxymethylbenzoate, 25

Phenol **24** (263 mg, 0.565 mmol) was dissolved in anh dichloromethane (6 mL) and *N,N'*-diisopropylethylamine (DIPEA) (0.30 mL, 1.60 mmol) was added at rt. The reaction mixture was cooled down to 0°C, and bromomethyl methyl (MOMBr) ether (0.10 mL, 1.13 mmol) was slowly added. The ice-water bath was removed after 10 min, and the reaction allowed to warm up to rt and stirred for 18 h. After this time, starting material was still present by TLC analysis, so the above procedure was repeated and the reaction left for another 18 h. The reaction was quenched with satd aq sodium hydrogen carbonate (40 mL), and extracted with ethyl acetate (3x40 mL). The combined organic layers were washed with water (50 mL), then brine (50 mL), dried over anhydrous sodium sulfate, filtered and concentrated *in vacuo*. Purification by FCC [petroleum ether-diethyl ether (80:20)→(70:30)] of the crude residue afforded MOM ether **25** (170 mg, 60%) as a colourless oil.

$[\alpha]^{20}$ –29.3 (*c* 1.1, $CHCl_3$); *v*max(film)/cm^{-1} 2984, 2938, 1663, 1369; ^{1}H NMR (400 MHz; $CDCl_3$) δ: 0.00 (6H, s), 0.82 (9H, s), 1.26 (3H, s), 1.36 (3H, s), 2.40-2.58 (2H, m), 3.45 (3H, s), 3.63-3.71 (2H, m), 3.80 (3H, s), 3.89 (3H, s), 4.09-4.15 (1H, m), 4.18-4.23 (1H, m), 5.13 (2H, s), 6.21-6.31 (1H, m), 6.42 (1H, d, *J* = 15.7 Hz), 6.59 (1H, d, *J* = 2.2 Hz), 6.69 (1H, d, *J* = 2.2 Hz); ^{13}C NMR (100 MHz; $CDCl_3$) δ: -5.3, -5.2, 18.4, 25.7, 26.0, 28.3, 33.4, 52.2, 55.5, 56.3, 62.0, 77.3, 77.8, 95.9, 100.0, 103.8, 108.1, 116.6, 129.2, 130.6, 137.7, 155.7, 161.4, 168.5; MS (EI) *m/z* 197 $[M]^+$; HRMS *m/z* 197.0772 (197.0784 calcd for $C_8H_{14}NaO_4$, M^+).

Methyl 2-[(*E*)-3-((4*S*,5*R*)-5-hydroxymethyl-2,2-dimethyl-[1,3]dioxolan-4-yl)-propenyl]-4-methoxy-6-methoxymethylbenzoate, 26

MOM ether **25** (373 mg, 0.730 mmol) was dissolved in anh tetrahydrofuran (5 mL) and cooled down to 0°C before the addition of *tetra*butylammonium fluoride (1.5 mL, 1.46 mmol). After 10 min, the ice-water bath was removed and the reaction was allowed to warm up to rt. After 1.5 h, the reaction was di-

luted with ethyl acetate (10 mL), and water (10 mL) was added. The organic layer was separated, dried over anhydrous sodium sulfate, filtered and concentrated *in vacuo*. Purification by FCC [petroleum ether-ethyl acetate (30:70)] of the crude residue afforded alcohol **26** (268 mg, 93%) as an off white oil.

$[\alpha]^{20}$ –6.0 (*c* 1.1, $CHCl_3$); *v*max(film)/cm^{-1} 2988, 2937, 1601, 1433; ^{1}H NMR (400 MHz; $CDCl_3$) δ: 1.35 (3H, s), 1.48 (3H, s), 2.37-2.47 (1H, m), 2.49-2.58 (1H, m), 3.45 (3H, s), 3.67 (2H, t, *J* = 5.8 Hz), 3.79 (3H, s), 3.88 (3H, s), 4.20 (1H, q, *J* = 5.8 Hz), 4.28 (1H, dt, *J* = 8.0, 5.8 Hz), 5.13 (2H, s), 6.18 (1H, ddd, *J* = 15.6, 7.8, 6.1 Hz), 6.43 (1H, d, *J* = 15.6 Hz), 6.59 (1H, d, *J* = 2.1 Hz), 6.69 (1H, d, *J* = 2.1 Hz); ^{13}C NMR (100 MHz; $CDCl_3$) δ: 25.4, 28.0, 33.2, 52.2, 55.4, 56.1, 61.3, 76.3, 77.8, 94.7, 100.6, 103.6, 108.2, 116.2, 128.8, 129.6, 137.3, 155.5, 161.2, 168.3; MS (EI) *m/z* 396 $[M]^+$; HRMS *m/z* 396.1787 (396.1784 calcd for $C_{20}H_{28}O_8$, M^+).

(*R*)-(-)-Pent-4-yn-2-ol, 28

A stirred suspension of lithium acetylide ethylenediamine complex (5.7 g, 62.0 mmol) in anh dimethylsulfoxide (110 mL) at 0°C was treated dropwise with *R*-(+)-propylene oxide, **27** (3.6 mL, 51.6 mmol). The reaction was then allowed to warm up to rt, where it was stirred for 48 h. The suspension was poured onto ice (100 mL), and extracted with diethyl ether (4x80 mL). The combined ether extracts were washed with brine (6x30 mL), water (2x30 mL) and dried over anhydrous magnesium sulfate. Careful evaporation of the solvent at atmospheric pressure yielded the crude alcohol **28** which was taken on without any purification.

$[\alpha]^{22}$ –18.0 (*c* 1.0, $CHCl_3$); *v*max(film)/cm^{-1} 3340 , 3301, 2360; ^{1}H NMR (400 MHz; $CDCl_3$) δ: 1.20 (3H, d, *J* = 6.0 Hz), 2.10 (1H, t, *J* = 2.7 Hz), 2.33 (1H, ddd, *J* = 16.0, 5.3, 2.7 Hz), 2.42 (1H, ddd, *J* = 16.0, 6.2, 2.7 Hz), 4.02-4.04 (1H, m); ^{13}C NMR (100 MHz; $CDCl_3$) δ: 24.7, 32.8, 67.2, 71.1, 85.1; MS (CI) *m/z* 67 $[M\text{-}OH]^+$; HRMS *m/z* 67.0550 (67.0548 calcd for C_5H_7, MOH^+).

1-Methoxy-4-((*R*)-1-methyl-but-3-ynyloxymethyl)-benzene, 29

NaH (60% dispersion in mineral oil, 2.27 g, 56.7 mmol) was diluted with anhydrous dimethylformamide (65 mL) and cooled down to 0°C. A solution of the freshly generated crude alcohol **28** (4.34 g, 51.6 mmol) in anhydrous dimethylformamide (65 mL) was added, and the resulting reaction mixture was stirred for 15 min. *p*-Methoxybenzyl chloride (10.5 mL, 77.4 mmol) was then added to the reaction and the mixture was allowed to warm up to rt and stirred for 17 h. The solution was then poured onto brine (400 mL) and extracted with diethyl ether (3x100 mL). The combined organic layers were concentrated under reduced pressure, washed with brine (300 mL), dried over anhydrous magnesium sulfate, filtered and the solvent concentrated. Purification by FCC [petroleum ether-ethyl acetate (95:5)] of the crude residue afforded PMB ether **29** (4.13 g, 40%) as a colourless oil.

$[\alpha]^{19}$ +11.2 (*c* 1.1, $CHCl_3$); *v*max (film)/cm^{-1} 2253, 911, 739; ^{1}H NMR (400 MHz; $CDCl_3$) δ: 1.32 (3H, d, *J* = 6.0 Hz), 2.04 (1H, t, *J* = 2.6 Hz), 2.38 (1H, ddd, *J* = 16.6, 7.0, 2.6 Hz), 2.52 (1H, ddd, *J* = 16.6, 4.9, 2.6 Hz), 3.70 (1H, sext, *J* = 6.0 Hz), 3.86 (3H, s), 4.53 (2H, s), 6.91 (2H, d, *J* = 8.6 Hz), 7.31 (2H, d, *J* = 8.6 Hz); ^{13}C NMR (100 MHz; $CDCl_3$) δ: 19.5, 26.0, 55.3, 69.9, 70.3, 72.8, 81.3, 113.8, 129.2, 130.6, 159.1; MS (EI) *m/z* 204.04 $[M]^+$; HRMS *m/z* 204.1146 (204.1150 calcd for $C_{13}H_{16}O_2$, M^+).

Methyl 2-((*E*)-3-{(4*S*,5*R*)-5-[(*S*)-1-hydroxy-5-(4-methoxybenzyloxy)-hex-2-ynyl]-2,2-dimethyl-[1,3]dioxolan-4-yl}-propenyl)-4-methoxy-6-methoxymethylbenzoate, 31

A solution of alkyne **29** (82.4 mg, 0.403 mmol) in anhydrous tetrahydrofuran (2 mL) was treated with ethyl magnesium bromide (0.13 mL, 0.378 mmol) at rt and the resulting solution was stirred for 5.5 h. Whilst the above deprotonation was being carried out, a -78°C solution of oxalyl chloride (0.25 mL, 0.504 mmol) in anhydrous tetrahydrofuran (3 mL) was added to dimethylsulfoxide (70 µL, 1.00 mmol). After stirring for 30 min, a solution of alcohol **26** (100 mg, 0.252 mmol) in anhydrous tetrahydrofuran (1.5 mL) was added to the dimethylsulfoxide solution, and stirring continued for 1 h at -78°C. After this time, triethylamine (0.28 mL, 2.02 mmol) was added, and the reaction was allowed to warm up to rt. After 30 min the reaction was cooled back down to -78°C and a solution of the deprotonated alkyne was added. The mixture was then allowed to warm up to rt overnight. The reaction was then quenched with saturated aqueous ammonium chloride (10 mL) and extracted with ethyl acetate (3x20 mL). The combined organic layers were dried over anhydrous sodium sulfate, filtered and concentrated *in vacuo*. Purification by FCC [petroleum ether-ethyl acetate (50:50)] of the crude residue afforded propargylic alcohol **31** (113 mg, 75%) as a pale yellow oil, and as an inseparable mixture of diastereoisomers;

$[\alpha]^{25}$ +0.04 (*c* 0.9, $CHCl_3$). *v*max(film)/cm^{-1} 3434, 3019, 1720, 1602, 1215, 765, 669; ^{1}H NMR (400 MHz; $CDCl_3$) δ: 1.30 (3H, s), 1.38 (3H, s), 1.54 (3H, s), 2.39-2.78 (4H, m), 3.50 (3H, s), 3.60-3.70 (1H, m), 3.81 (3H, s), 3.83 (3H, s), 3.91 (3H, s), 4.20-4.30 (1H, m), 4.43-4.47 (1H, m), 4.45-4.55 (3H, m), 5.18 (2H, s), 6.23-6.29 (1H, m), 6.49 (1H, d, *J* = 15.7 Hz), 6.62 (1H, s), 6.71 (1 H, s), 6.89 (2H, d, *J* = 8.5 Hz), 7.27 (2H, d, *J* = 8.5 Hz); ^{13}C NMR (100 MHz; $CDCl_3$) δ: 19.8, 25.5, 26.5, 27.6, 31.0, 33.3, 52.3, 55.3, 55.5, 56.2, 62.1, 70.4, 72.9, 73.1, 79.7, 80.4, 84.5, 94.8, 100.7, 103.8, 108.6, 113.8, 128.7, 129.2, 129.3, 130.2, 137.6, 155.6, 161.3, 168.0, 171.1; MS (FAB) *m/z* 599.3 $[M+H]^+$; HRMS *m/z* 599.2843 (599.2857 calcd for $C_{33}H_{43}O_{10}$, $M+H^+$).

Methyl 4-methoxy-2-((*E*)-3-{(4*S*,5*S*)-5-[(*S*)-5-(4-methoxybenzyloxy)-1-triisopropylsilanyloxy-hex-2-ynyl]-2,2-dimethyl-[1,3]dioxolan-4-yl}-propenyl)-6-methoxymethylbenzoate, 32

Propargylic alcohol **31** (113 mg, 0.188 mmol) was dissolved in anhydrous dimethylformamide (2 mL), imidazole (38 mg, 0.566 mmol) added and the solution was stirred until homogenous. Triisopropylsilyl chloride (0.05 mL, 0.226 mmol) was then added at rt and the reaction left to stir overnight. The reaction mixture was diluted with ethyl acetate (10 mL) and quenched with water (10 mL). The organic layer was separated, extracted with water (3x30 mL), dried over anhydrous sodium sulfate, filtered and concentrated *in vacuo*. Purification by FCC [petroleum ether-ethyl acetate (50:50)] of the crude residue afforded TIPS ether **32** (114 mg, 80%) as a yellow oil.

$[\alpha]^{19}$ –2.2 (*c* 1.13, $CHCl_3$); *v*max(film)/cm^{-1} 2943, 2866, 1725, 1601, 1513, 1266, 1215, 1154, 757; ^{1}H NMR (400 MHz; $CDCl_3$) δ: 1.01-1.12 (21H, m), 1.29 (3H, s), 1.37 (3H, s), 1.50 (3H, s), 2.34 (1H, dd, *J* = 16.5, 7.6 Hz), 2.51-2.74 (3H, m), 3.46 (3H, s), 3.61-3.67 (1H, m), 3.76 (3H, s), 3.81 (3H, s), 3.88 (3H, s), 4.09-4.29 (2H, m), 4.48 (2H, d, *J* = 6.7 Hz), 4.53 (1H, d, *J* = 6.4 Hz), 5.14 (2H, s), 6.22-6.31 (1H, m), 6.40 (1H, dd, *J* = 15.6, 4.4 Hz), 6.60 (1H, s), 6.69 (1H, d, *J* = 3.3 Hz), 6.87 (2H, t, *J* = 6.8 Hz), 7.22-7.27 (2H, m); ^{13}C NMR (100 MHz; $CDCl_3$) δ: 12.3, 17.7, 19.8, 25.7, 26.5, 27.8, 34.0, 52.2, 55.3, 55.5, 56.2, 62.8, 70.3, 73.2, 77.3, 80.5, 80.7, 83.7, 94.8, 100.7, 103.6, 108.5, 109.0, 113.8, 128.3, 129.2, 130.9, 131.0, 137.1, 156.1, 159.0, 161.2, 168.0; MS (FAB) *m/z* 777.7 $[M+Na]^+$; HRMS *m/z* 777.4019 (777.4012 calcd for $C_{42}H_{62}NaO_{10}Si$, $M+Na^+$).

Methyl 4-methoxy-2-((*E*)-3-{(4*S*,5*S*)-5-[(*Z*)-(*R*)-5-(4-methoxy-benzyloxy)-1-triisopropylsilany-

loxy-hex-2-enyl]-2,2-dimethyl-[1,3]dioxolan-4-yl}-propenyl)-6-methoxymethylbenzoate, 33

A solution of TIPS ether **32** (59 mg, 77.9 µmol) in methanol (1.5 mL) was treated with a catalytic amount of $Pd/BaSO_4$ catalyst and poisoned with quinoline (0.01 mL, 97.3 µmol). The flask was evacuated, and after purging three times with hydrogen gas *via* a balloon, the mixture was stirred under an atmosphere of hydrogen for 2h at rt. At this time, TLC analysis deemed the reaction complete, and the solution was filtered through a pad of Celite® to remove the catalyst and the solvent concentrated *in vacuo*. Purification by FCC [petroleum ether-ethyl acetate (60:40)] of the crude residue afforded alkene **33** (53 mg, 89%) as a pale yellow oil.

$[\alpha]^{26}$ –2.4 (*c* 0.9,$CHCl_3$); *v*max(film)/cm^{-1} 2943, 2865, 1729, 1602, 1513; ^{1}H NMR (400 MHz; $CDCl_3$) δ: 1.04 (3H, s), 1.09 (18H, s), 1.23 (3H, d, *J* = 6.1 Hz), 1.32 (3H, s), 1.42 (3H, s), 2.22-2.69 (4H, m), 3.45 (3H, s), 3.56-3.60 (1H, m), 3.77 (3H, s), 3.81 (3H, s), 3.87 (3H, s), 3.92-4.16 (2H, m), 4.36-4.52 (2H, m), 4.61-4.70 (1H, m), 5.14 (2H, s), 5.48-5.68 (2H, m), 6.25-6.31 (1H, m), 6.43-6.47 (1H, m) 6.59 (1H, s), 6.74 (1H, s), 6.85 (2H, d, *J* = 6.7 Hz), 7.24-7.27 (2H, m); ^{13}C NMR (100 MHz; $CDCl_3$) δ: 12.8, 17.7, 19.8, 25.6, 27.0, 27.5, 34.0, 52.1, 55.3, 55.5, 56.2, 68.1, 70.1, 74.3, 77.6, 80.3, 94.8, 100.7, 108.2, 108.3, 113.8, 117.0, 128.2, 129.2, 130.9, 131.0, 131.2, 132.3, 142.4, 155.5, 159.1, 161.2, 168.7; MS (FAB) *m/z* 779.7 $[M+Na]^+$; HRMS *m/z* 779.4168 (779.4169 calcd for $C_{42}H_{64}NaO_{10}Si$,$M+Na^+$).

Methyl 2-{(*E*)-3-[(4*S*,5*S*)-5-((*Z*)-(*R*)-5-hydroxy-1-triisopropylsilanyloxy-hex-2-enyl)-2,2-dimethyl-[1,3]dioxolan-4-yl]-propenyl}-4-methoxy-6-methoxymethylbenzoate, 34

PMB ether **33** (148 mg, 0.195 mmol) was dissolved in a mixture of dichloromethane (2 mL) and pH 7 buffer (2 mL), and cooled to 0°C. 2,3-Dichloro-5,6-dicyano-1,4-benzoquinone (58 mg, 25.4 µmol) was then added with vigorous stirring, and the reaction was allowed to warm up to rt overnight. After this time, the reaction was re-cooled back down to 0°C, and further 2,3-dichloro-5,6-dicyano-1,4-benzoquinone (58 mg, 25.4 µmol) was added. After allowing the reaction to warm up to rt overnight again, the reaction mixture was diluted with dichloromethane (15 mL) and quenched with saturated aqueous sodium hydrogen carbonate (15 mL). The aqueous layer was separated and extracted with dichloromethane (3x40 mL). The combined organic layers were washed with brine (40 mL), dried over anhydrous Na_2SO_4, filtered, and concentrated *in vacuo*. Purification by FCC [petroleum ether-ethyl acetate (60:40)] of the crude residue afforded alcohol **34** (108 mg, 87%) as a yellow oil.

$[\alpha]^{26}$ –0.03 (*c* 1.4, $CHCl_3$); *v*max(film)/cm^{-1} 3450, 2942, 2865, 1721, 1598, 1150; ^{1}H NMR (400 MHz; $CDCl_3$) δ: 0.93 (3H, s), 1.06 (18H, s), 1.18 (3H, d, *J* = 6.1 Hz), 1.31 (3H, s), 1.46 (3H, s), 2.12-2.18 (1H, m), 2.23-2.32 (1H, m), 2.45-2.63 (2H, m), 3.45 (3H, s), 3.80 (3H, s), 3.86 (3H, s), 3.96-4.02 (1H, dd, *J* = 8.9, 5.6 Hz), 4.22-4.29 (1H, m), 4.73 (1H, t, *J* = 8.5 Hz), 5.12 (2H, s), 5.56-5.67 (2H, m), 6.23-6.30 (1H, m), 6.40 (1H, d, *J* = 15.7 Hz), 6.57 (1H, d, *J* = 2.2 Hz), 6.71 (1H, d, *J* = 2.2 Hz); ^{13}C NMR (100 MHz; $CDCl_3$) δ: 12.9, 18.2, 23.8, 26.1, 28.1, 29.7, 34.4, 38.7, 52.1, 55.4, 56.2, 66.7, 77.7, 80.3, 94.8, 100.7, 103.7, 108.8, 116.5, 128.7, 129.9, 130.4, 133.8, 137.5, 155.5, 161.2, 168.4; MS (EI) *m/z* 636.6 $[M]^+$; HRMS *m/z* 636.3699 (636.3694 calcd for $C_{34}H_{56}O_9Si$, M^+).

2-{(*E*)-3-[(4*S*,5*S*)-5-((*Z*)-(*R*)-5-Hydroxy-1-triisopropylsilanyloxy-hex-2-enyl)-2,2-dimethyl-[1,3]dioxolan-4-yl]-propenyl}-4-methoxy-6-methoxymethylbenzoic acid, 35

Methyl ester **34** (79 mg, 0.124 mmol) was dissolved in ethanol (1.5 mL) and 2 *N* potassium hydroxide (1.5 mL) was added dropwise. A colour change from yellow to orange was observed after the addition of base. The reaction was heated under reflux for 48 h whereafter it was cooled down to rt and diluted with water (10 mL). The solution was acidified to pH 1-2 using 6 *N* hydrochloric acid, and was then extracted with ethyl acetate (3x15 mL). The combined organic layers were washed with water (20 mL), then brine (20 mL), dried over anhydrous sodium sulfate, filtered and concentrated *in vacuo*. Purification by FCC [petroleum ether-ethyl acetate (80:20)] of the crude residue afforded *seco*-acid **35** (47 mg, 61%) as a thick, pale orange oil.

$[\alpha]^{21}$ –0.1 (*c* 1.0, $CHCl_3$); *v*max(film)/cm^{-1} 3447, 2941, 2866, 2359, 1724, 1604, 1248, 1155, 1041; ^{1}H NMR (400 MHz; $CDCl_3$) δ: 0.94 (3H, s), 1.02 (18H, s), 1.21 (3H, d, *J* = 6.1 Hz), 1.30 (3H, s), 1.47 (3H, s), 2.08-2.45 (2H, m), 2.80-3.00 (2H, m), 3.52 (3H, s), 3.82 (3H, s), 3.94-4.20 (3H, m), 4.63-4.67 (1H, m), 5.23 (2H, s), 5.59-5.71 (2H, m), 6.20-6.27 (1H, m), 6.42-6.48 (1H, m), 6.51 (1H, s), 6.72 (1H, s); ^{13}C NMR (100 MHz; $CDCl_3$) δ: 12.5, 18.2, 23.5, 26.0, 28.0, 29.7, 34.4, 38.7, 55.4, 56.5, 67.0, 77.5, 80.3, 95.3, 100.7, 105.5, 108.9, 114.0, 128.7, 130.2, 131.0, 133.0, 139.7, 156.2, 161.7, 169.0; MS (FAB) *m/z* 645.6 $[M+Na]^+$; HRMS *m/z* 645.3436 (645.3437 calcd for $C_{33}H_{54}NaO_9Si$, $M+Na^+$).

(2*E*,11*Z*)-(5*S*,9*S*,14*S*)-20-Methoxy-18-methoxymethyl-7,7,14-trimethyl-10- triisopropylsilanyloxy-6,8,15-trioxa-tricyclo[15.4.0.05,9]henicosa-1(21),2,11,17,19-pentaen-16-one, 36

Seco-acid **35** (45 mg, 72.4 µmol) was dissolved in anhydrous toluene (10 mL) and triphenylphosphine (38 mg, 145 µmol) was added at rt. The mixture was stirred until homogenous, and then the reaction mixture was cooled down to 0°C, at which stage diethyl azodicarboxylate (20 µL, 145 µmol) was added dropwise. The ice-water bath was removed after 5 min and after a further 5 min, TLC analysis showed the total consumption of starting material. The solvent was then carefully evaporated *in vacuo*. Purification by FCC [petroleum ether – ethyl acetate (70:30)] of the crude residue afforded lactone **36** (31 mg, 73%) as a yellow oil.

$[\alpha]^{21}$ –1.6 (*c* 1.0, $CHCl_3$); *v*max(film)/cm^{-1} 3439, 2941, 2866, 1725, 1606, 1249; ^{1}H NMR (400 MHz; $CDCl_3$) δ: 0.80 (3H, s), 0.99 (18H, s), 1.18 (3H, s), 1.26 (3H, s), 1.42 (3H, s), 2.02-2.70 (4H, m), 3.38 (3H, s), 3.70 (3H, s), 3.75-4.05 (3H, m), 4.73-4.76 (1H, m), 5.08 (2H, s), 5.47-5.76 (2H, m), 6.07-6.13 (1H, m), 6.25-6.29 (1H, m), 6.45 (1H, s), 6.51 (1H, s); ^{13}C NMR (100 MHz; $CDCl_3$) δ: 12.8, 18.3, 23.8, 26.4, 28.9, 29.7, 30.4, 38.7, 55.5, 56.2, 68.2, 77.2, 81.4, 94.7, 100.6, 104.9, 107.8, 113.7, 128.8, 130.1, 131.0, 132.5, 137.8, 156.1, 161.4, 167.8; MS (FAB) *m/z* 627 $[M+Na]^+$; HRMS *m/z* 627.3324 (627.3329 calcd for $C_{33}H_{52}NaO_8Si$, $M+Na^+$).

(2*E*,11*Z*)-(5*S*,9*R*,14*S*)-10-Hydroxy-20-methoxy-18-methoxymethyl-7,7,14-trimethyl-6,8,15-trioxa-tricyclo[15.4.0.05,9]henicosa-1(21),2,11,17,19-pentaen-16-one, 37

Lactone **36** (31 mg, 51.9 µmol) was dissolved in anhydrous tetrahydrofuran (2 mL) and the solution was cooled down to 0°C. Tetrabutylammonium fluoride (1.0 M in THF, 0.1 mL, 0.104 mmol) was added, and the ice-water bath removed after 10 min. After 1 h, the reaction mixture was diluted with ethyl acetate (10 mL) and water (10 mL). The organic layer was separated and dried over anhydrous sodium sulfate, filtered and concentrated *in vacuo*, to afford alcohol **37** which was used without any further purification.

$[\alpha]^{24}$ –2.8 (*c* 1.0, $CHCl_3$); *v*max(film)/cm^{-1} 3360, 2922, 2851, 1720, 1661, 1468, 1155, 1043; ^{1}H NMR (400 MHz; $CDCl_3$) δ: 1.16 (3H, s), 1.22 (3H, s), 1.40 (3H, s), 2.00-2.63 (4H, m), 3.38 (3H, s), 3.68 (3H, s), 3.75-4.00 (3H, m), 4.33-4.37 (1H, m), 5.10 (2H, s),

5.47-5.76 (2H, m), 5.90-6.10 (2H, m), 6.45 (1H, s), 6.51 (1H, s); ^{13}C NMR (100 MHz; $CDCl_3$) δ: 23.8, 26.5, 28.9, 29.7, 30.4, 38.8, 55.4, 56.2, 68.2, 77.2, 81.4, 94.7, 100.6, 104.9, 107.9, 113.7, 128.8, 130.1, 131.0, 132.5, 137.8, 156.1, 161.4, 168.0.

(2*E*,11*Z*)-(5*S*,9*S*,14*S*)-20-Methoxy-18-methoxymethyl-7,7,14-trimethyl-6,8,15-trioxa-tricyclo[15.4.0.05,9]henicosa-1(21),2,11,17,19-pentaene-10,16-dione, 38

Pyridinium chlorochromate (29 mg, 132 μmol) was dissolved in anhydrous dichloromethane (1.6 mL), and a solution of alcohol **37** (30 mg, 66 μmol) in anhydrous dichloromethane (1.6 mL) was added at rt. The reaction was stirred for 18 h, and then decanted into a clean flask and the residue washed with dichloromethane (2x10 mL). The solvent was concentrated *in vacuo* and the residual material diluted with diethyl ether (20 mL). The suspension was filtered through cotton wool to remove the chromium salts. The ethereal component was washed with 1 M sodium hydroxide (15 mL), then brine (15 mL) and dried over anhydrous Na_2SO_4, filtered and concentrated *in vacuo* to leave an orange/brown residue. Purification by FCC [petroleum ether – ethyl acetate (50:50)] of the crude residue afforded protected LL-Z1640-2 **38** (10 mg, 34%).

$[\alpha]^{22}$ –0.16 (*c* 1.0, $CHCl_3$); *v*max(film)/cm^{-1} 2952, 1760, 1599, 1019, 979; ^{1}H NMR (400 MHz; $CDCl_3$) δ: 1.24 (6H, s), 1.32 (3H, d, *J* = 12.6 Hz), 2.45-2.70 (4H, m), 3.43 (3H, s), 3.75 (3H, s), 4.41-4.43 (1H, m), 4.53-4.56 (1H, m), 4.63 (1 H, d, *J* = 7.8 Hz), 5.08-5.15 (1H, m), 5.29 (2H, s), 5.43-5.48 (1H, m), 6.01-6.05 (1H, m), 6.30-6.54 (2H, m), 6.54 (1H, m).

References

1. Ellestad, G.A.; Lovell, F. M.; Perkinson, N. A.; Hargresves, R.T.; McGahren, W. J. *J. Org. Chem.* **1978**, *43*, 2339.
2. Takehara, K.; Sato, S.; Kobayashi, T.; Maeda, T. *Biochem. Biophys. Res. Comm.* **1999**, *257*, 19.
3. (a) Giese, N. A.; Lokker, N. Int. Pat. WO9613259; (b) Nonomiya-Tsuji, J.; Kajino, T.; Ono, K.; Ohtomo, T.; Matsumoto, M.; Shiina, M.; Mihara, M.; Tsuchiya, M.; Matsumoto, K. *J. Biol. Chem.* **2003**, *278*, 18485
4. Lu, L.; Zhang, X.; Tong, H.; Zhang, W.; Xu, P.; Qu, S. *Front. Pharmacol*. **2017**, *8*, 789.
5. (a) Kastelic, T.; Schnyder, J.; Leutwiler, A.; Traber, R.; Streit, B.; Niggli, H.; MacKenzie. A.; Cheneval, D. *Cytokine* **1996**, *8*, 751; (b) Elford, P. R.; Dixon, A. K.; MacKenzie, A. R.; Leutwiler, A.; Schnyder, *J. Pharmacol. Comm.* **1996**, *7*, 301.
6. (a) Moulin, E.; Barluenga, S.; Winssinger, N. *Org. Lett.* **2005**, *7*, 5637; (b) Garbaccio, R. M.; Danishefsky, S. J. *Org. Lett.* **2000**, 2, 3127; (c) Garbaccio, R. M.; Stachel, S. J.; Baeschlin, D. K.; Danishefsky, S. J. *J. Am. Chem. Soc*. **2001**, *123*, 10903; (d) Tichkowsky, I.; Lett, R. *Tetrahedron Lett.* **2002**, *43*, 3997; (e) Tichkowsky, I.; Lett, R. *Tetrahedron Lett.* **2002**, *43*, 4003; (f) Lampilas, M.; Lett, R. *Tetrahedron Lett.* **1992**, *33*, 773.
7. (a) Tatsuta, K.; Takano, S.; Sato, T.; Nakano, S. *Chem. Lett.* **2001**, 172; (b) Selles, P.; Lett, R. *Tetrahedron Lett.* **2002**, *43*, 5621; (c) Selles, P.; Lett, R. *Tetrahedron Lett*. **2002**, *43*, 4627.
8. Miyatake-Ondozabal, H.; Barret, A. G. M. *Org. Lett.* **2010**, *12*, 5573.
9. Fakhouri, L.; El-Elimat, T.; Hurst, D. P.; Reggio, P. H.; Pearce, C. J.; Oberlies, N. H.; Croatt, M. P. Bioorg. *Med. Chem*. **2015**, *23*, 6993.
10. LeClair, C. A.; Boxer, M. B.; Thomas, C. J.; Maloney, D. J. *Tetrahedron Lett.* **2010**, *51*, 6852.
11. Jana, N.; Nanda, S. New. *J. Chem.* **2018**, *42*, 17803.
12. Robertson, M. N., Ph.D. Thesis, University of Glasgow, **2009**
13. Stille, J. K. *Angew*. *Chem.* **1986**, *98*, 504.
14. Barbat, J.; Gelas, J.; Horton, D. *Carbohydrate Res*. **1983**, *116*, 312.
15. Geng, X. D.; Danishefsky, S. J. *Org. Lett.* **2004**, *6*, 413.
16. Schultz, A. G.; Green, N. J. *J. Am. Chem. Soc.* **1992**, *114*, 1824.

A chemist's journey to subduction

Peter Hodder

School of Government, Victoria University of Wellington *and* HodderBalog Social and Scientific Research, Wellington (email: *peter.hodder@vuw.ac.nz; peterh@hodderbalog.co.nz*)

Keywords: *earthquakes, phase transitions, subduction, mantle, citation analysis*

Authors's note: Inspiration for the title of this article came from a book of personal geological field-trips in San Francisco: Wahrhaftig, C. *A streetcar to subduction and other plate tectonic trips by public transport in San Francisco.* American Geophysical Union, Washington D.C., revised edition, 1984.

Many years ago, when I was a raw chemistry graduate with an interest in geology, I noticed that geology research papers often included tables of the chemical composition of rocks and minerals, but the chemical data shown were rarely used to shed light on the geological processes involved. This was one reason why I was attracted to a suggested MSc thesis project that sought to provide a chemical basis for the mechanism of earthquakes.

The starting point of the project was the suggestion that minerals in the mantle might take different forms at different depths. For example, the mineral olivine [$(Mg, Fe^{(II)})_2SiO_4$], a principal component of rock then inferred to characterise the earth's upper mantle, might change its structure from one in which the oxygen atoms are arranged in a hexagonal close-packed type of lattice to a structure in which the oxygens are arranged in a cubic close-packed type of lattice that is characteristic of the mineral spinel [Al_2MgO_4] at the higher temperature and pressures of greater depths in the mantle. Initial experiments that appeared to demonstrate the reaction's feasibility (Table 1) were confirmed two decades later, and continued to attract attention.

Table 1. Experimental olivine → spinel transitions at pressures and temperatures characteristic of the mantle*

Compound	Temperature (°C)	Pressure (kb)	% increase in density
Mg_2SiO_4	530	100 ± 15	4.7%
	600	130 ± 20	> 9%
	900	170	10.3%
Fe_2SiO_4†	600	38 ± 3	10.5%

* Data from reference 2

† Volume change differs little between Fe- and Mg- compounds, and indicates volume change is attributed largely to the change from hexagonal close-packing to cubic close packing of the lattice of oxygen atoms

My research question was essentially whether mineralogical transitions such as that from olivine to spinel, with its decrease in volume could occur under non-equilibrium conditions and fast enough to produce a shock wave. Although the research was intended to be a theoretical study, in an effort to include an experimental component to this research, I – unbeknown to my supervisor – tried bursting balloons in a bath of green jelly, hoping that a shock wave resulting from the collapse of the balloon might be preserved in the gelatinous medium (Fig. 1).

The MSc project identified several chemical systems in which phase transitions and polymorphic transitions occurred with changes in volume that might occur sufficiently rapidly to generate a shock wave and suggested that such an approach might be applicable to reactions and phase transitions in the mantle. Shock wave generation required the transforming phases to become metastable, but a way to achieve this in the geological environment was not immediately obvious – at least to chemists.

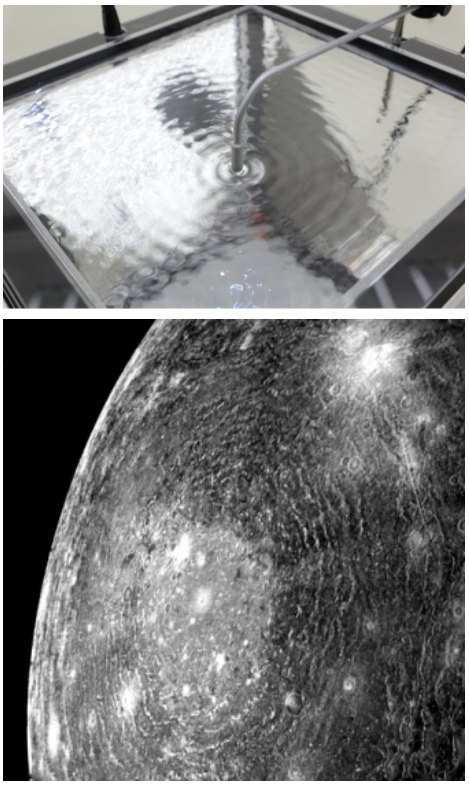

Fig. 1. An experimental wave ripple tank (A) was the inspiration for an experiment which, it was hoped, would lead to the preservation of ripples of the propagation of the shock wave, akin to later images of Valhalla, a multi-ring feature 3800 km in diameter resulting from an impact on Callisto, one of Jupiter's moons (B) (https://ase.tufts.edu/cosmos/view_picture.asp?id=1181), but the idea was as 'dead in the water' as is portrayed in The Death of Marat, by Jacques-Louis David, 1793; see: https://www.independent.co.uk/arts-entertainment/art/great-works/great-works-the-death-of-marat-by-jacques-louis-david-1793-9035080.html.

The then embryonic research area of plate tectonics provided the answer: subduction. This is the physical process by which oceanic crust returns to the earth's mantle – as the slab of oceanic crust is pulled or pushed into the mantle (by forces unknown at the time). Subduction provided an increase in temperature and pressure to which

the minerals in the rocks were subjected. This might enable a mineral to become metastable: a reaction or phase transition might alleviate the metastability condition and release a shock wave, and was expressed at the time thus:

"… in the mantle there exists an anomalous zone of the order of 100 km thick whose upper surface is approximately defined by a highly active seismic zone which dips … beneath the island arc and extends to depths of about 700 km. … the structure suggests the lithosphere is thrust or dragged down beneath the arc and hence implies a certain mobility for the lithosphere elsewhere. This possibility suggests in turn new approaches to a wide variety of problems [including] the nature of the earthquake mechanism."

However, the mechanism of the olivine-spinel transition has continued to attract the experimental attention of others, some with no better results than mine. For example, one review simply sidestepped the issue by suggesting that the mechanism was probably dependent on the experimental conditions, while another noted that "neither a nucleation and growth model nor a martensite model is verified by the experimental results".

My later theoretical calculations for a variety of candidate reactions suggested that only the reaction shown in Eq. 1 satisfied the criteria for production of a shock wave, but even so the calculated shock pressure was very low – much lower than the confining pressure of the rocks!

$$Mg_{48}Si_{34}O_{85}(OH)_{62} + 135MgSiO_3 \rightarrow 45Mg_2SiO_4 + 31Mg_3Si_4O_{10}(OH)_2 \quad \text{(Eq. 1)}$$

antigorite + clinoenstatite → forsterite + talc

Although not recognised as significant at the time, other candidate reactions considered generated water, for example Eqs. 2-4:

$$Al_2Si_4O_{10}(OH)_2 + 6AlO(OH) \rightarrow 4Al_2SiO_5 + 4H_2O \quad \text{(Eq. 2)}$$

pyrophyllite + diaspore → kyanite + water

$$Al_2Si_4O_{10}(OH)_2 \quad Al_2SiO_5 + 3SiO_2 + H_2O \quad \text{(Eq. 3)}$$

pyrophyllite + kyanite → quartz + water

$$KFe_3(AlSi_3O_{10})(OH)_2 + 3SiO_2 \rightarrow KAlSi_3O8 + 3FeSiO_3 + H_2O \quad \text{(Eq. 4)}$$

annite + quartz → K-feldspar + ferrosilite + water

Only much later was the release of the bound water from such minerals considered to be a potential lubricant to the subduction process. Such processes came to be envisaged as contributing to the dynamics of subduction itself: pulling or pushing the slab downwards, as much as a potential mechanism for earthquake generation.

As it turned out, the location of subduction zones in those places where planes of earthquake locations descending into the mantle are prominent – the so-called Wadati-Benioff zones, named after the two scientists – Hugo Benioff and Kiyoo Wadati – who first identified them, has ensured that interest in the idea of phase changes and reactions that were accompanied by a change in volume being an earthquake source mechanism has persisted (Fig. 2).

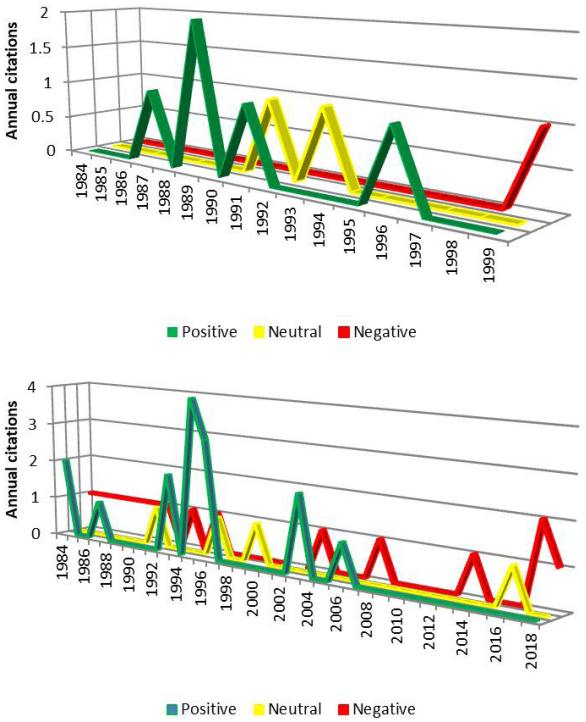

Fig. 2. Citation trends I. Upper: The few citations of Hodder (1984) [reference 9] show that most citations are positive about the idea of phase transitions being an earthquake source mechanism. Lower: The 36 citations of Pennington (1983) (reference 11) show a broadly similar trend. On both plots the highest earliest peaks are positive citations.

The resurgence of interest shown in Fig. 2 by the peaks in the mid-1990s is also apparent in the publication date distribution of references across the four sections of a 1996 compilation of papers, each section of which includes papers relevant to a different depth range in the mantle. The distribution plots are shown in Fig. 3, with the features of the plots compared in Table 2.

One of the more recent flurries of interest in the topic has been the proposing of

"transformational faulting in a wedge of olivine-rich peridotite that is likely to persist metastably in coldest plate interiors to depths as great as 690 km. Predictions based on this deep structure of mantle phase changes are consistent with the global depth distribution of deep earthquakes, the maximum depths of earthquakes in individual subduction zones, and key source characteristics of deep events".

This particular piece of research has been extensively cited (see Fig. 4; 400 citations from 1991, as at June 2019), the peaks suggesting at least one upsurge in interest compared with earlier research which tended to focus on earthquakes at relatively shallow depths (e.g. reference 12, for which 36 citations from 1983 are recorded, as at June 2019; see Fig. 2).

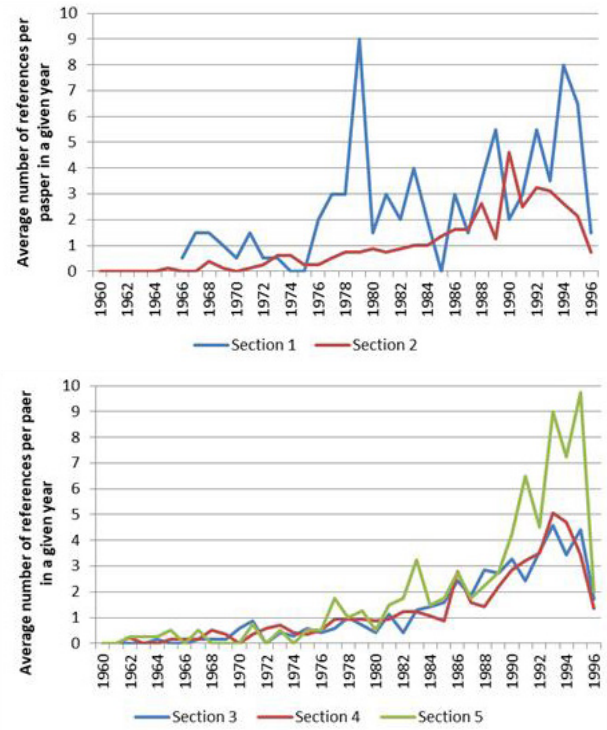

Fig. 3. Variation of average number of references per paper in sections of a compilation of research papers related to subduction (reference 12). The four sections in order of increasing depth in the mantle are: Section 1, What goes in; Section 2, 'The first squeeze'; Section 3, 'The big squeeze: Back from the pressure cooker'; Section 4, 'The big squeeze: From beneath the arc'; Section 5, 'The biggest squeeze: Slab structure and deep-focus earthquakes'

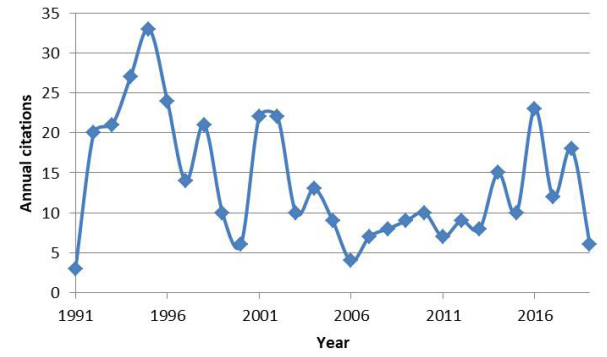

Fig. 4. Citation trends II. The over 400 citations of Kirby *et al.* (1991, reference 13). The initial peak at 1995 is followed by others in 2001-2002 and in 2016 which suggests a continual resurgence of interest in the idea.

The continued downward progression of the subducted oceanic crust into the mantle leads to some of it melting, providing the source of at least some of the material erupted at volcanoes, such as those in New Zealand's Taupo Volcanic Zone (Fig. 5).

In portraying these rocks as being derived from such a source, diagrammatic representations in public media often rely on simple physical models of diapiric uprise of molten rock through overlying materials. My own thoughts in this area (Fig. 6 – upper) were stimulated by a paper which included experiments that used engine oil rising from a slotted container into a glass aquarium filled with water (Fig. 6 – lower), rather like a two dimensional lava lamp. My reading of this paper prompted my performing a number of messy demonstrations in front of university extension classes and at open days.

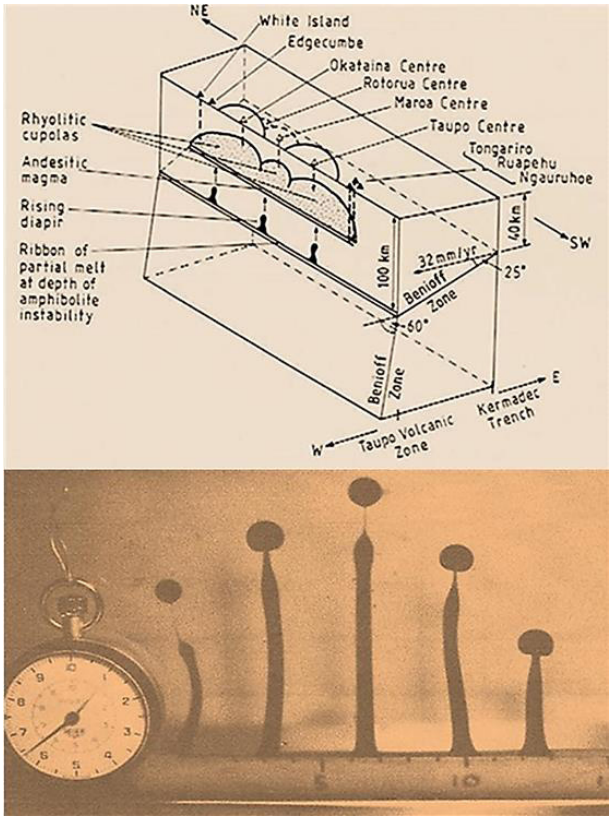

Fig. 6. Volcanoes of the Taupo Volcanic Zone envisaged (upper) as forming from diapirs rising from a melt at the top of the subduction zone (Hodder 1983; reference 15), inspired by a physical model sketched by the author in 1982 (lower), based on an idea developed by Marsh (1979, reference 16).

Table 2. Resurgence of interest in earthquake-related research in subducting slabs*

Increasing depth in mantle	Section	Number of papers in each section	Number of references in each section	Principal peak in distribution†
	1	2	161	1979
	2	8	254	1990
	3	7	319	1993
	4	14	637	1993
	5	4	270	1995
All sections		35	1650	

*compiled from reference 13; titles for sections are listed in caption to Fig. 3

† For each section these are easily seen in Fig. 3; there are also other subsidiary peaks, interpreted as other 'flurries' of interest

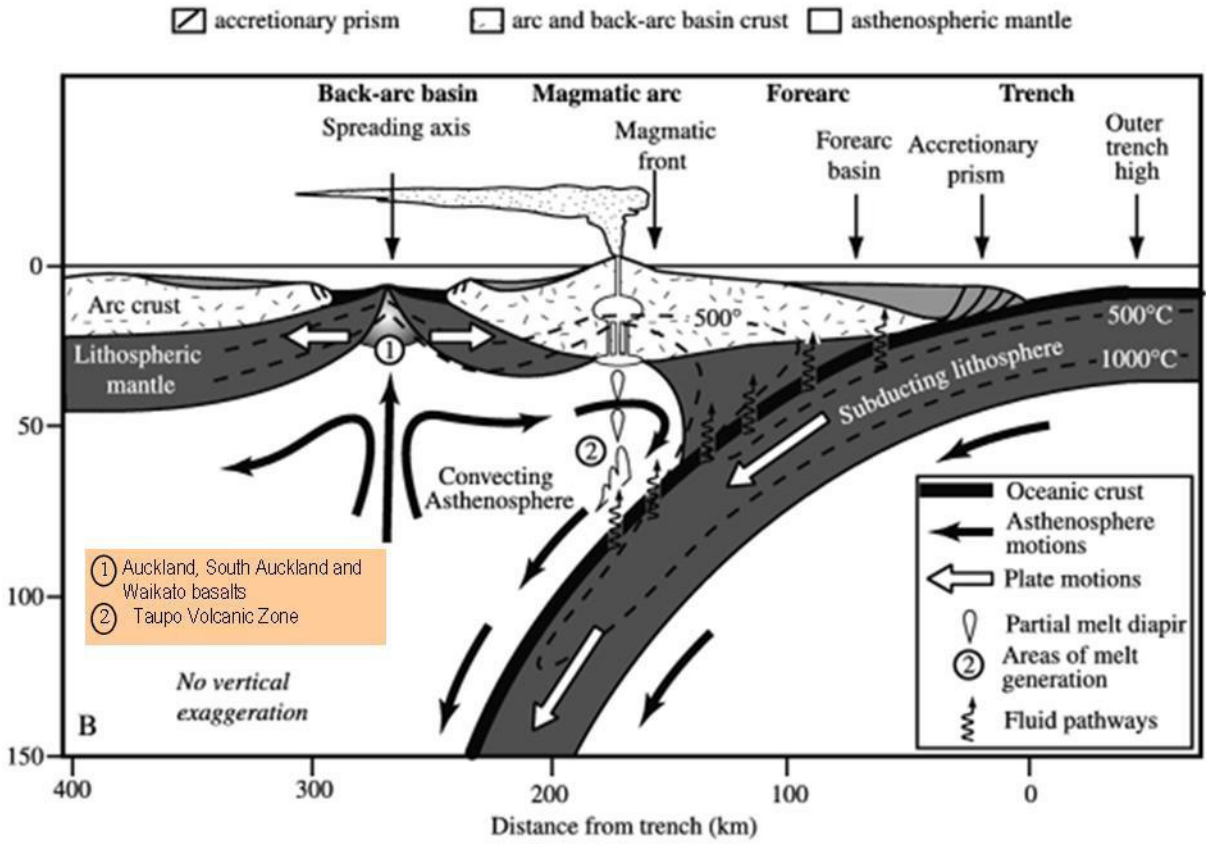

Fig. 5. General features of a subduction zone, with location of Taupo Volcanic Zone and the Auckland, South Auckland and Waikato basalts identified. Adapted from Stern (2002, Fig. 1b, reference 14).

In fact, there is considerable chemical variation in the rocks of the Taupo Volcanic Zone, suggesting either successive mixing of batches of variably fractionated magmas (i.e., molten rocks) and/or different materials being involved in the formation of magma during the lifetime of volcanic arcs formed above subduction zones. John Holden's cartoon from the 1970s shows a deity sweeping materials into the top of the subduction zone (Fig. 7). This predated the recognition that volcanic rocks of the central North Island show chemical evidence of greywackes – a prominent sedimentary rock in New Zealand – in their bulk geochemistry, although in the more evolved rocks (e.g., rhyolitic lavas), this may have been caused by magmas having "originated below crustal formations and both have become contaminated by greywacke through which they passed to reach the surface". As perhaps might be expected, Holden's 'sweeping' has meant that there are "variable amounts of subduction-derived fluid within the melting region of the basalts".

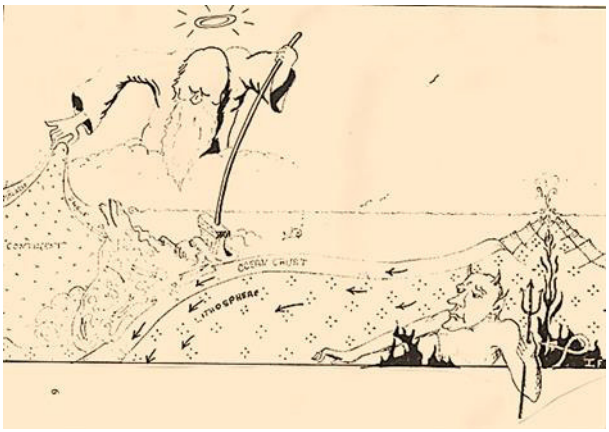

Fig. 7. The prospect of a 'mash-up' in a subduction zone like that shown in Fig. 5: sediments being incorporated into the down-going slab. The volcano with the devil underneath is 'managing' either an oceanic hotspot or an oceanic spreading centre. Cartoon by John Holden (reference 19).

Fig. 5 also notes the possibility of volcanics being derived from greater depths than those that typify the Taupo Volcanic Zone. These are represented in the North Island by the basaltic volcanoes of Northland, Auckland and South Auckland, and the Waikato, and have a different chemical composition from those in the central North Island, attesting to a different source and/or melt generation processes. The burgeoning availability of major and trace element compositional data in the 1980s led to the development of many 'geochemical discrimination diagrams' which sought to assign tectonic settings to volcanic rocks or provenances to sedimentary rocks and selected minerals. The widespread but potentially inappropriate use of geochemical discrimination diagrams prompted a cautionary paper, by one of their first proponents, while the vexed question of the reliability of the boundaries of the fields on such diagrams also drew comment. As might be anticipated, the tedium of the calculations involved eventually led to software being developed.

How deep could subduction go? Fig. 8 shows subduction progressing to the core-mantle boundary, an idea that had been suggested at least as early as 1982. It was a short step from this to associating deep subduction with previously identified geochemical 'heterogeneities' and

'low velocity' geophysical anomalies deep in the mantle. My response to this idea was to speculate on the possibility of a large mantle heterogeneity being an influence on the chemistry of basaltic volcanism across the South Pacific.

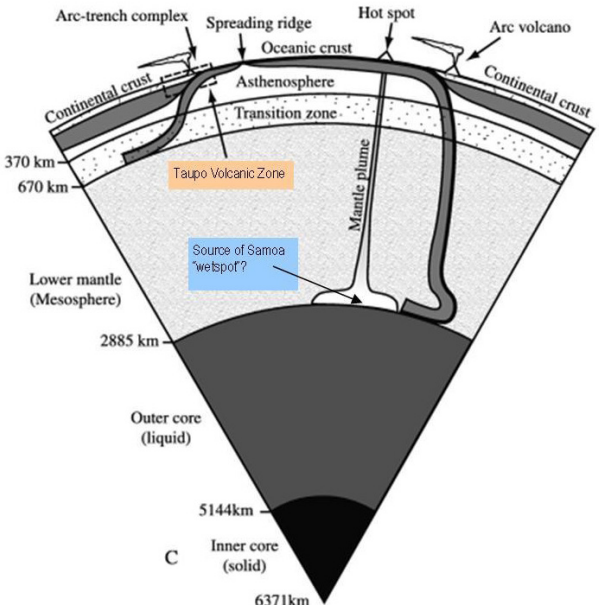

Fig. 8. Deep subduction: a possible source of non-mantle material for 'hotspots' and 'wetspots'. Adapted from Stern (2002, Fig. 1c, reference 14).

Many intraplate volcanoes (e.g., the Hawaiian Islands) are associated with mantle plumes which rise from the core-mantle boundary far from the boundaries of tectonic plates: these have long been referred to as 'hot spots'. Deep subduction has the potential to provide an additional complexity to mantle plumes. As an example, for a plume beneath Samoa, the mixing of lower mantle materials with deeply subducted materials has been inferred, by comparing the compositions of basalt and the 'upper continental crust' with which it may have been contaminated. This contamination was identified by comparisons of 'spidergrams', in which the ratios of concentrations of incompatible elements (including the lanthanides) to concentrations of the same elements in a standard rock (typically meteoritic) are compared across a variety of rocks, as shown in Fig. 9.

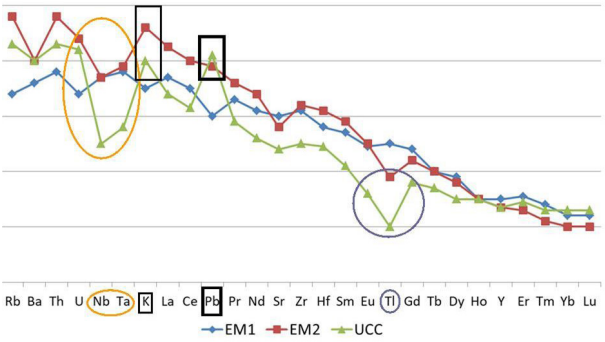

Fig. 9. Spidergram for Samoan unenriched basalt (EM1); enriched basalt (EM2), with upper crustal component (UCC). Vertical axis is the ratio of concentration in sample to that in primitive mantle. The similarity of negative anomalies for Nb, Ta and Tl and the similarity of positive anomalies for K and Pb argue for a common source for these elements. Redrawn from Fig. 2 in reference 35.

A subsequent review has commented, "They argue … that the Samoan plume contains a significant component of anciently subducted, continent-derived sediment, and it is difficult to imagine any alternative scenario."

Deep subduction may also transport minerals that still contain bound water deep into the mantle; the dehydration of these materials may be responsible for earthquakes, whereby "a deep-crustal earthquake scenario where a high-pressurized fluid phase plays a double role by causing both seismic failure through the embrittlement effect and facilitating eclogitization of the metastable anhydrous gabbro". Moreover, at the depths where the subducted material finally melts there might still be sufficient volatiles for 'wet' magma to be one explanation for the occurrence of mantle 'wet spots'.

From earthquakes to 'wet spots', my involvement with subduction lasted some twenty years, continually suggesting new lines of enquiry; some of these I followed up, but others I was unable or unwilling to pursue. In concluding, I can do no better than concur with the 16th century poet Alexander Pope's expression of similar sentiments in an extract from his poem, *An essay on criticism*:

"Fired at first youth with what the Muse imparts,
In fearless youth we tempt the heights of Arts,
While from the bounded level of our mind
Short views we take, nor see the lengths behind;
But more advanced, behold with strange surprise
New distant scenes of endless science rise!"

References and Notes

1. Ringwood, A.E.; Major, A. *Earth Planetary Sci. Lett.* **1966**, 1 (4), 241-245.
2. Bina, C.R.; Wood, B.J. *J. Geophys. Res. Solid Earth*, **1987**, *92* (B6), 4853-4866. Thermodynamic parameters for the Ge analogue have also been determined; see: Ross, N.L.; Navrotsky, A. *Phys. Chem. Mineral.* **1987**, *14* (5), 473-481.
3. Bina, C.R.; Helffrich, G. *J. Geophys. Res.* **1994**, *99* (B8), 15853-15860.
4. Barton, A.F.M.; Hodder, A.P.W. *Chem. Rev.* **1973**, *73*(2), 127-139. The model advanced in this paper was later applied to the freezing of supercooled water in: Hodder, A.P.W. *N. Z. J. Geol. Geophys.* **1976**, *19* (6), 821-826.
5. Barton, A.F.M.; Hodder, A.P.W.; Wilson, A.T. *Nature* **1971**, *234* (5327), 293-294.
6. Oliver, J.; Isacks, B. *J. Geophys. Res.* **1967**, *72* (16), 4259-4275.
7. Green, H.W. *Geophys. Res. Lett.* **1984**, *11* (9), 817-820.
8. Hamaya, N.; Akimoto, S. *Physics Earth Planet. Interiors* **1982**, *29* (1), 6-11. A martensitic transformation was not supported by: Vaughan, P.J.; Green, H.W.; Coe, R.S. *Nature* **1982**, *298*, 357-358.
9. Hodder, A.P.W. *Earth Planet. Sci. Lett.* **1984**, *34*, 221-225.
10. Sornette, D. In *Earthquake thermodynamics and phase transformations in the Earth's interior* (Eds.: Teisseyre, R.; Eugeniusz Majewski E.), Cambridge University Press: Cambridge, 2018.
11. Pennington, W.D. *Science* **1983**, *220*, 1045-1047; see also: Fukao, Y.; Hori, S.; Ukawa, M. *Nature* **1983**, *303*, 413-415.
12. Bebout, G.E.; Scholl, D.W.; Kirby, S.H.; Platt, J.P. (Eds.). *Geophysical Monograph* **1996**, *96*.

13. Kirby, S.H.; Durham, W.B.; Stern, L.A. *Science* **1991**, *252* (5003), 215-225; see also: Kirby, S.H.; Stein, S.; Okal, E.A.; Rubie, D.C. *Rev. Geophys.* **1996**, *34* (2), 261-306.
14. Stern, R.J. *Rev. Geophys.* **2002**, *40* (4), 3-1 – 3-38.
15. Hodder, A.P.W. *Chem. Geol.* **1983**, *38*, 275-285.
16. Marsh, B.D. *J. Geol.* **1979**, *87*, 687-713.
17. Hodder, A.P.W. *J. Geol. Ed.* **1983**, *31*, 193-197.
18. Hodder, A.P.W. *Chem. Geol.* **1985**, *48*, 3-16. This paper drew inspiration from: Dickinson, W.R. *Geology* **1975**, *3*, 53-56.
19. Holden, J.C.; Vogt, P.R. *EOS Trans. Am. Geophys. Union* **1977**, *58*, 573-580.
20. Carter, L.; Carter, R.M.; McCave, I.N.; Gamble, J. *Geology* **1996**, *24* (8), 735-738.
21. Hiess, J. Cole, J.W.; Spinks, K.D. *N. Z. J. Geol. Geophys.* **2007**, *50*, 327-342; see also: Blattner, P.; Reid, F. *Geochim. Cosmochim. Acta* **1982**, *46* (8), 1417-1429.
22. Rooney, T.O.; Deering, C.D. *Geology* **2014**, *42* (1), 3-6.
23. Numerous examples of geochemical discrimination diagrams are given in Rollinson, H. *Using Geochemical Data: Evaluation, Presentation, Interpretation.* Longman: Harlow, UK, 1993, pp. 171-214.
24. One of probably hundreds of papers that have used this approach to assign tectonic environments is: Hodder, A.P.W. *Tectonophysics* **1984**, *101*, 293-318.
25. An example of this approach is: Winefield, P.R.; Nelson, C.S.; Hodder, A.P.W. *Carbonate and Evaporites* **1996**, *11* (1), 19-31.
26. Pearce, J.A. In *Trace Element Geochemistry of Basaltic Rocks: Applications for Massive Sulfide Exploration* (Ed.: Wyma, D.A), *Geological Association of Canada Short Course Notes* **1996**, *12*, 79-113.
27. Vermeesch, P. *Geochem. Geophys. Geosys. G³* **2006**, *7* (6), Q06017, doi:10.1029/2005GC001092.
28. An example is: Janoušek, V.; Farrow, C.M.; Erban, V. *J. Petrol.* **2006**, *47* (6), 1255-1259.
29. Hofmann, A.W.; White, W.M. *Earth Planet. Sci. Lett.* **1982**, *57*, 421-436.
30. Hart, S.R. *Nature* **1984**, *309*, 753-757.
31. Dziewonski, A.M.; Anderson, D.L. *Am. Sci.* **1984**, *72*, 483-494; Dziewonski, A.M. *J. Geophys. Res.* **1984**, *89*, 5929-5952.
32. Hodder, A.P.W. *Tectonophysics* **1987**, *134*, 263-272.
33. Hodder, A.P.W. *Tectonophysics* **1988**, *156*, 145-165.
34. Frey, F.A.; Clague, D.A. *Earth Planet. Sci. Lett.* **1983**, *66*, 337-355. For a recent review see: Haase, K.M.; Beier, C.; Kemner, F. *Frontiers Earth Sci.* **2019**, 04 January 2019, https://doi.org/10.3389/feart.2018.00242. The 'classical' compilation of papers on this topic for the New Zealand region is: Johnson, R.W. *Intraplate volcanism in Eastern Australia and New Zealand*. Cambridge University Press: Cambridge, 1989.
35. Jackson, M.G.; Hart, S.R.; Koppers, A.A.P.; Staudigel, H.; Konter, J.; *et al*. *Nature* **2007**, *448* (7154), 684–687.
36. White, W.M. *Ann. Rev. Earth Planet. Sci.* **2010**, 38: 133-160; see also: Lawrence, J.F.; Wysession, M.E. *Geophys.l Monograph* **2006**, *168*. 251-261.
37. Lund, M.G.; Austrheim, H. *Tectonophysics* **2003,** *372* (1-2), 59-83.
38. Métric, N.; Zanon, V.; Créon, L.; Hildenbrand, A.; Moreira, M.; Marques. F.O. *J. Petrol.* **2014**, 55 (2), 377–393.
39. Pope, Alexander. *An Essay on Criticism* **1711**. London: Publisher unknown.

Determining tectonic settings using geochemical discrimination diagrams

Peter Hodder

School of Government, Victoria University of Wellington *and* HodderBalog Social and Scientific Research, Wellington (email: *peter.hodder@vuw.ac.nz*; *peterh@hodderbalog.co.nz*)

Keywords: *geochemical discrimination diagrams, basalt, andesite, granites, sediments, spidergrams*

The development of plate tectonics yielded a number of settings where plates are drawn/pushed apart (e.g., mid-ocean ridges and continental rifts), or pushed together (collisional zones), or where one plate is pushed/pulled under another – the subduction zone – leading to island arcs or continental arcs. All these lead to particular types of volcanoes; complemented by those that form far away from extensional or compressional boundaries from mantle plumes. The essentials of these settings are shown schematically in Fig. 1.

There are chemical differences between the materials erupted from these various settings and various combinations of elements have been used to 'discriminate' between them. Combinations of elements in rocks of 'known' tectonic setting are used to define a diagram that can then be applied to to predict the likely tectonic setting of other rocks, as shown schematically in Fig. 2.

Reality can be a bit more complicated than this because not all rocks have unique tectonic settings (i.e., parts of the fields can overlap), and there are subsets of tectonic settings; magma compositions can be affected by fractionation and melting processes; and rocks can be affected by post-emplacement weathering and alteration by fluids.[1] In addition, there is an inherent assumption that the types of tectonic settings in the distant past resemble those currently observed.[2] In addition, the boundaries between the fields are not always well constrained.[3]

The development of such diagrams coincided with the availability of improved methods of determining the chemical composition of rocks and minerals, resulting in 25 different diagrams applicable to basalts, shown in Table 1;[4-17] one diagram applicable to andesites (generally a fractionated form of basalt), also shown in Table 1;[18] six diagrams applicable to granites (Table 2);[2,19-20] and eight diagrams applicable to various types of sedimentary rocks (Table 3).[21-24] These diagrams involve a variety of elements, for which the inter-relationships between them are displayed as two-dimensional plots, triangular diagrams, or discriminant functions. In some diagrams a tectonic setting may be uniquely associated with a particular field on the diagram ((identified with the symbol ● in Tables 1-3); in others the tectonic setting is not identified with a single field (identified with the symbol ❍ in

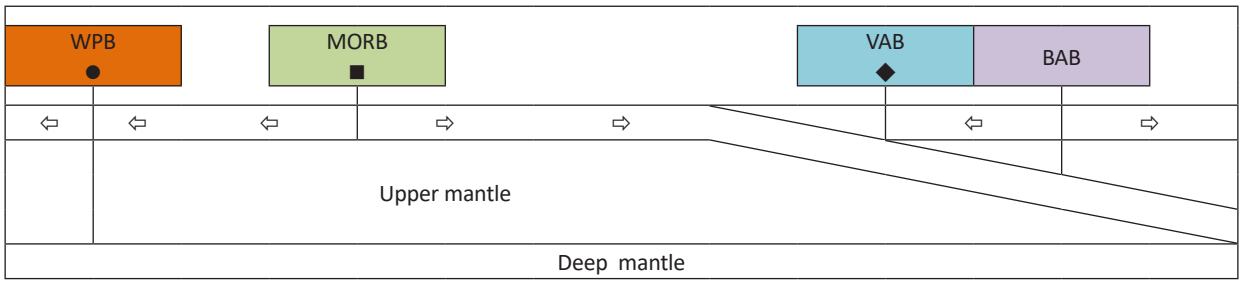

Fig. 1. Schematic diagram of the major plate tectonic settings - and will be helpful when reading Table 1. Arrows show plates moving either side of a Mid-Oceanic Ridge, which erupts basalts (MORBs), the most common of which are 'normal' (N-MORB); if there is mixing between N-MORB and the basalts of Oceanic Island Basalts (OIB), the rocks are referred to as E-MORBs. At the left, the plate moves over a mantle hot-spot or plume, from which are erupted 'Within Plate Basalts' (WPB), which include OIBs from Oceanic Islands, and alkali basalts (which contain high amounts of sodium and have other diagnostic chemical features too). To the right of the mid-ocean ridge, the plate is subducted. At a depth of about 100 km 'Volcanic Arc Basalts' (VAB) - and associated magmas - are formed. These may occur in island settings ('Oceanic Island Arc', OIA), or at continental margins (where shoshonitic basalts and andesites, which are potassium-rich can occur; while in some cases, from greater depths 'behind' the arc, 'Back Arc Basalts' (BAB) are erupted, often in an environment of minor rifting, shown as the small diverging arrows at the right-hand side of the diagram.

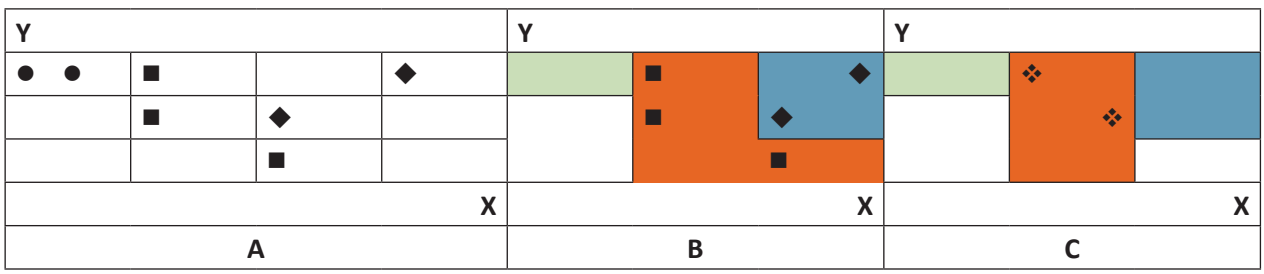

Fig. 2. Development and use of geochemical discrimination diagrams. A. Using compositions of rocks of known tectonic setting (●, ■, ◆) to 'train' a geochemical discrimination diagram to show fields appropriate to particular settings (B), and then using it (C) to suggest the tectonic setting of an 'unknown' rock (❖). The variables (X, Y) on the diagram can be individual element compositions, or functions that are some combination of elemental compositions (e.g., ratios, sums, or more complex discriminant functions).

Table 1. Geochemical discrimination diagrams for basalts and andesite

Ref: No. of citations	Diagram	Mid-ocean ridge basalt (MORB)				Back-arc basin tholeiites (BAB)	Within-plate basalts (WPB)								Volcanic-arc basalts (VAB)						Reliability index (RI)
		Unspecified	N-MORB	E-MORB	Transitional		Unspecified	Alkali	Tholeiitic	Transitional	Ol tholeiites	Ol alkalu basalts	Continental tholeiites	Continentalalkali basalt	Unspecified	Island-arc tholeiites	Continental-arc	Oceanic-arc	Calc-alkal-ine basalts	Shoshonitic bassallts	
4: 4153	Ti-Zr-Y	❍					●									●❍			●❍		0.711
	Ti-Zr (linear)	❍●														●❍			●❍		
	Ti-Zr (logarithmic)	❍					❍											●❍			
	Ti-Zr-Sr	●																	●		
	Discr. fn. Ti-Zr-Y-Sr	●					●									●❍		❍	●❍		
5: 2893	Zr/Y – Zr	●❍		❍			●❍										❍	●❍			0.540
6: 2201	Th-Hf-Ta		●	❍				●	❍									●	●		0.800
7: 2028	T-V	❍				❍		●			●					●❍			❍		0.600
8: 2006	Zr-Nb-Y		❍	●				●❍	❍									❍			0.520
9: 1799	Ti/Y – Nb/Y	●❍					●	●	●	●								●❍			0.886
	Cr-Y	●❍					●❍											●			
	Cr – Ce/Sr	●❍					●❍											●			
	K2O/Yb – Ta/Yb	●❍					●❍	●	●	●						●			●	●	
10: 994	MnO-TiO2-P2O5	●						●			●								●		1.000
11: 885	TiO2 – Y/Nb	●❍						●❍					●								0.643
	Nb/Y – Zr/P2O5											●❍	●❍	●❍		❍					
12: 829	P2O5 - Zr							●	●												1.000
	TiO2 – Zr/P2O5							●	●												
13: 483	MgO-FeO-Al2O3	●									❍		❍				❍				0.500
	TiO2-K2O-P2O5	❍										❍	●								
14: 431	DIscr fn (major) -I	●					●									❍			❍	●	0.844
	Discr.fn (major)-II	●														●			●	●	
15: 406	Zr/Y – Ti/Y						●								●						1.00
16: 64	K2O-H2O	●				●❍					●					❍		●			0.800
17: 63	La-Y-Nb		●	●									●			●❍	●		●❍		0.914
18*: 251	La/Yb – Sc/Ni*																●	●❍			0.700

● unique field (i.e. basalts of only one type of setting plots in this region of the diagram); ❍ mixed field (i.e. basalts of more than one setting may plot in this region of the diagram)

*andesite

N-MORB: normal MORB; E-MORB: isotopically-enriched N-MORB

Table 2. Geochemical discrimination diagrams for granites

Ref: No. of citations	Diagram	ORG*	WPG	VAG	COLG		RI
					Syn	*Post*	
2: 8070	Nb-Y	●	●	❍	❍		0.913
	Ta-Yb	●	●	●	●		
	Rb-(Y+Nb)	●	●	●	●		
	Rb-(Yb+Ta)	●	●	●	●		
19: 1501	Hf-Rb/10-3Ta	●	●❍	❍	❍		0.838
	Hf-Rb/30-3Ta		●	●	●	●	
20: 525	Rb/Zr – Nb or Y†			●			1.000

* Granite types and settings: ORG, Ocean-ridge granites; WPG, Within-plate granites; VAG, Volcanic arc granites; COLG, Collisional granites – subdivided to 'Syn-tectonic granites', associated with continent-continent collision or continent-arc collision; and 'Post-tectonic granites', associated with continent-continent collision (see ref. 2)

● unique field; (i.e., granites of only one type of setting plots in this region of the diagram)

❍ mixed field (i.e., granites of more than one setting may plot in this region of the diagram)

† Values of both ratios increase with maturity

Table 3. Geochemical discrimination diagrams for sedimentary rocks

Ref: No. of citations	Diagram	Clastic sediments*				Sandstone-mudstone†				Greywacke*				RI
		PM	ACM	CIA	OIA	QSP	MIP	IIP	FIP	PM	ACM	CIA	OIA	
21: 2079	La-Th-Sc									❍	❍	●	●	0.825
	Th-Sc-Zr/10									●	●	●	●	
22: 1735	Discr.fn (major)	●	●	●	●									0.950
	TiO2-(Fe2O3+MgO)	●	●	●	●									
	(Al2O3/SiO2)-(Fe2O3+MgO)	●❍	●❍	●	●									
23: 1435	Log(K2O/Na2O)-SiO2	●	●		●									1.000
24: 1135	Discriminant function -I‡					●	●	●	●					1.000
	Discriminant function -II‡					●	●	●	●					

* Clastic sediments or greywackes and settings; **PM:** passive margin, **ACM:** active continental margin, **CIA:** continental island arc, **OIA:** oceanic island arc.

● unique field; (i.e., sediments of only one type of setting plots in this region of the diagram).

❍ mixed field (i.e., sediments of more than one setting may plot in this region of the diagram).

† Provenance signatures; **QSP:** quartzose sedimentary provenance, **MIP:** mafic (i.e., similar composition to basalt) igneous provenance, **IIP:** intermediate igneous provenance (i.e., similar composition to andesite), **FIP:** felsic igneous provenance.

‡ These functions include the compositions of major elements only.

Table 4. Average reliability index for diagrams used for determining tectonic settings of different rock types

Diagrams using …	Basalts	Andesite	Granites	Sediments
… Major elements	0.786			0.983
… Trace elements	0.761	0.700	0.875	0.823
All diagrams	0.768	0.700	0.875	0.944

Tables 1-3), while in others the tectonic setting is associated with both a particular field, and a shared field (identified with the symbol ●❍ in Tables 1-3). On this basis each diagram can be given a reliability index, calculated as shown in Eq. 1:

$$\textit{Reliability index } (RI) = [N_{\bullet} + (0.7{*}N_{\bullet\circ}) + (0.3{*}N_{\circ})]/[N_{\bullet} + N_{\bullet\circ} + N_{\circ}] \quad \text{(Eq. 1)}$$

where N is the number of analyses of rocks in the various tectonic settings.

Table 4 shows that the average reliability index is slightly higher for sedimentary rocks than it is for granites, for the latter of which the average reliability exceeds that for basalts and andesites. Although twenty years have passed since many of these diagrams were first introduced, they continue to be cited – some extensively. However, there is no obvious relationship between the reliability index in the diagrams with the total number of citations, the citations per year, or the year of publication.

For the most highly cited paper that introduced a geo-

chemical discrimination diagram for basalts,[4] andesites,[18] granites,[2] and sedimentary rocks,[21] the publication dates for those 100 papers that cited it that were themselves the most highly cited subsequently were used to calculate an annual citation rate, from which five-year moving averages of citations rates were determined, as shown in Fig. 3.

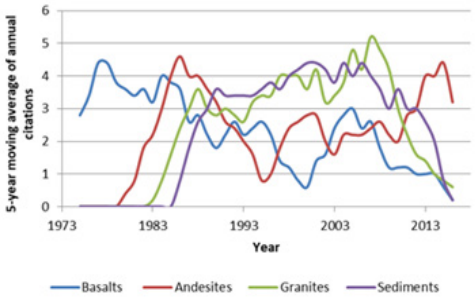

Fig. 3. Five-year moving average of annual citations for the 100 most cited of the most cited paper relating to discrimination diagrams for each of basalts (ref. 4), andesites (ref. 18), granites (ref. 2), and sedimentary rocks (ref. 21).

Fig. 3 suggests that the use of diagrams for discriminating basalts peaked in 1977 (four years after publication of ref. 4 in 1973) and has been essentially in decline thereafter, perhaps because of the increasing use of 'spidergrams' – either of the lanthanades alone[25] or a wider group of incompatible elements[26] – in characterising these rocks.

For each chemical element of the spidergram, the ratio of concentration of the element in the rock is normalised to (i.e. divided by) the concentration of the element in the primordial mantle. The estimated values of the primordial mantle composition have varied over time: three commonly used examples were published in 1979,[27] 1989,[28] and 1995;[29] the publication dates for those 100 papers that cited each of those papers[27-29] that were themselves the most highly cited subsequently were used to calculate an average annual citation rate. Fig. 4 compares this rate with that for the basalt curve from Fig. 3.

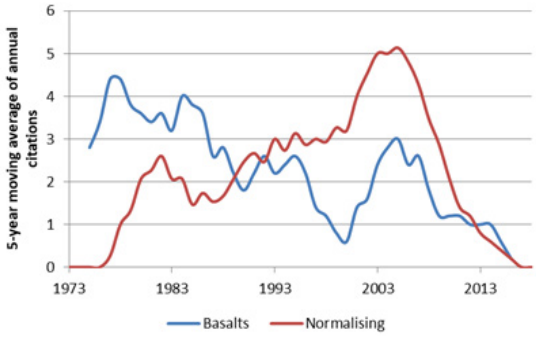

Fig. 4. Basalts plot from Fig. 3 compared with the average citation rate for a selection of highly cited papers that suggest normalising coefficients for spidergrams (refs. 27-29). The trend of the former declines while the latter increases from the late 1970s to the early 2000s.

The use of diagrams for andesites peaked in 1986 (five years after publication of ref. 18 in 1981), but has increased in use thereafter. In contrast, citations of the diagrams for granites and sedimentary rocks have both continued to increase until the mid-2000s, but have declined thereafter.

Although it is clear that the heyday of geochemical discrimination diagrams has passed, it is perhaps a testament to Julian Pearce's original concept of the diagrams that their use has continued for so long. His work was acknowledged by his receipt of the Murchison Medal from The Geological Society in 2014.[30]

References and notes

1. Arculus, J. *J. Volcanology Geotherm. Res.* **1987**, *32*, 1-12.
2. Pearce, J.A.; Harris, N.B.W.; Tindle, A.G. *J. Petrology* **1984**, *25*, 956-983. For a readable account of how plate tectonics has changed over time, see: Nield, T. *Supercontinent: Ten Billion Years in the Life of Our Planet*. Granta: London, 2007.
3. Vermeesch, P. *Geochem. Geophys. Geosyst. G³* **2006**, *7* (6), Q06017, doi:10.1029/2005GC001092. For a wider perspective, see: Hoefs, J. Geochemical fingerprints: a critical appraisal. *Eur. J. Mineral.* **2010**, *22*, 3-15.
4. Pearce, J.A.; Cann, J.R. *Earth Planetary Sci. Lett.* **1973**, *19* (2), 290-300 [see Rollinson, 1993, Fig. 5.1].
5. Pearce, J.A.; Norry, M.J. *Contributions Mineral. Petrol.* **1979**, *69*, 33.47.
6. Wood, D.A. *Earth Planetary Sci. Lett.* **1980**, *50*, 11-30.
7. Shervais, J.W. *Earth Planetary Sci. Lett.* **1982**, *59*, 101-118.
8. Meschede, M. *Chem. Geol.* **1986**, *56*, 207-218.
9. Pearce, J.A. Trace element characteristics of lavas from destructive plate boundaries. In *Andesites* (Ed.: Thorpe, R.S.), *Andesites*, Wiley, Chichester, 1982, 525-548.
10. Mullen, E.D. *Earth Planetary Sci. Lett.* **1983**, *62*, 53-62.
11. Floyd, P.A.; Winchester, J.A. *Earth Planetary Sci. Lett.* **1975**, *27*, 211-218.
12. Winchester, J.A.; Floyd, P.A. *Earth Planetary Sci. Lett.* **1976**, *28* (3), 459-469.
13. Pearce, T.H.; Gorman, B.E.; Birkett, T.C. *Earth Planetary Sci. Lett.* **1977**, *36*, 121-132.
14. Pearce, J.A. *J. Petrol.* **1976**, *17*, 15-43.
15. Pearce, J.A.; Gale, G.H. *Geol. Soc. Special Pub.* **1977**, *7*, 14—24.
16. Muenow, D.W.; Garcia, M.O.; Aggrey, K.E.; Bednarz, U.; Schmincke, H.U. *Nature* **1990**, *343*, 159-161. (Erratum in *Nature* **1990**, *343*, 576.)
17. Cabanis, B.; Lecolle, M. *Comptes Rendus de l' Académie des Sciences, Série II* **1989**, *309*, 2023-2029.
18. Bailey, J.C. *Chem. Geol.* **1981**, *32*, 139-154.
19. Harris, N.B.W.; Pearce, J.A.; Tindle, A.G. In *Collision Tectonics. Special Publication of the Geological Society* (Eds.: Coward, M.P.; Reis, A.C.), 1986, *19*, 67-91.
20. Brown, G.C.; Thorpe, R.S.; Webb, P.C. *J. Geol. Soc. London* **1984**, *141*, 411-426.
21. Bhatia, M.R.; Crook, K.A.W. *Contributions Mineral. Petrol.* **1986**, *92*, 181-193.
22. Bhatia, M.R. *J. Geol.* **1983**, *91*, 611-627.
23. Roser, B.P; Korsch, R.J. *J. Geol.* **1986**, *94*, 635-650.
24. Roser, B.P.; Korsch, R.J. *Chem. Geol.* **1988**, *67*, 119-139.
25. O'Neill, H. St.C. *J. Petrol.* **2016**, *57* (8), 1463-1508.
26. Examples include: Marsh, J.S. Basalt geochemistry and tectonic discrimination within continental flood basalt provinces. *J. Volcanology Geothermal Res.* **1987**, *32* (1-3), 35-49; Hofmann, A.W. Chemical differentiation of the Earth: the relationship between mantle, continental crust and oceanic crust. *Earth Planetary Sci. Lett.* **1988**, *90* (3), 297-314.
27. Wood, D.A.; Tarney, J.; Varet, J. *et al. Earth Planetary Sci. Lett.* **1979**, *42*, 77-97 (which has been cited 307 times since its publication).
28. Sun, S.S.; McDonough, W.F. *Geol. Soc. London Special Pubs.* **1989**, *42*, 313-345 (which has been cited 31,235 times since its publication).
29. Donough, W.F.; Sun, S.S. *Chem. Geol.* **1995**, *120*, 223-153 (which has been cited 9,558 times since its publication).
30. The Geological Society. https://www.geolsoc.org.uk/About/awards-grants-and-bursaries/society-awards/murchison-medal (accessed 15/02/2020).

JOIN US!

INTERNATIONAL YOUNGER CHEMISTS NETWORK

Help us connect and empower younger chemists globally.

Communicate

Our goal is scientific and professional exchange across geographic and cultural boundaries.

Collaborate

We are focused on engaging young and early-career chemists to serve their specific needs.

Educate

Our network is growing, and we need your help in reaching chemists in your region or organization!

Mentor

We want to learn from you, support you, and empower your passion for chemistry.

How can we work together?

While we are eager to offer our resources and tools to your members, we also hope to add value to your organization by more broadly sharing relevant news, conferences, or information that you wish to disseminate. We look forward to working with you!

Learn more on our website: https://www.iycnglobal.com/